



Norwegian University
of Life Sciences

Master's Thesis 2021 60 ECTS

Faculty of Environmental Science and Natural Resource Management

Speciation and Source Identification of Radiocesium by Radiochemical Separation and QQQ-ICP-MS analysis

John Sebastian Hov

M-KB

Speciation and Source Identification of Radiocesium by Radiochemical Separation and QQQ-ICP-MS analysis

by

John Sebastian Hov

Faculty of Environmental Sciences and Natural Resource Management
Norwegian University of Life Sciences

December 2021

Acknowledgements

This thesis was carried out between August 2020 and December 2021 at the Faculty of Environmental and Natural Resource Management (MINA) at Norwegian University of Life Sciences (NMBU).

I would like to extend my greatest gratitude to my main supervisor, Estela Reinoso-Maset. Firstly, for making an interesting thesis for me. Secondly, for helping me through this thesis with your outstanding patience and excellent guidance. Your moral support has been incredible, and I will never forget our work and conversations together.

I would also like to extend my gratitude to my co-supervisors Karl Andreas Jensen and Ole Christian Lind. The conversations in the ICP-MS room with Karl Andreas will never be forgotten and I will cherish those happy memories. Your guidance, brilliance, and knowledge with the instruments at the lab is beyond this world. I also deeply appreciate the meetings with Ole and his valuable input and feedback throughout the thesis.

I would also like to thank my friends that has stood with me this year. Especially my friend Kristian Molvær Løndal, my former cohabitant and great friend. I deeply appreciate our conversations and our friendship.

These last years has been heavily affected by the Covid pandemic. It made everything more complicated towards the thesis. Luckily, I have friends and family in Ås and Bodø that helped with motivation.

Bodø, December 2021

John Sebastian Hov

Abstract

The Fukushima Daiichi Nuclear Power Plant (FDNPP) accident on March 11th, 2011, in Japan caused the release of radioactive fallout, including radioactive cesium (Cs), and contaminated the near field but also large areas 50-70 km from the reactors. The aim of this study was to optimize published methods for the radiochemical separation of radiocesium from environmental samples and measurement of ^{137}Cs and ^{135}Cs by triple quadrupole inductively coupled plasma mass spectrometry (QQQ-ICP-MS). This optimized method would then be applied to determine the $^{135}\text{Cs}/^{137}\text{Cs}$ isotopic ratio for source identification.

The method was optimized by testing and evaluating the different procedure steps. A simulated complex solution containing radiocesium was first used to evaluate: i) three techniques for separating Cs from AMP based on Cs recovery and convenience of work, and ii) the anion and cation resins based on ability to remove unwanted ions from solution. Using bulk soil samples from Fukushima, two acid mixtures were tested for extraction capacity of the microwave digestion. The resulting samples containing ^{137}Cs were then measured by QQQ-ICP-MS to check for Cs recovery and decontamination factor (DF) of unwanted ions. The measurements showed that the optimized method, using concentrate HNO_3 , 1 mg/mL AMP and a 0.45 μm syringe filter, resulted in 75-85% and ca. 100% Cs recovery in the digestion and radiochemical separation steps, respectively. Moreover, based on high DF for ICP-MS interfering elements, the anion resin step was excluded, thus reducing the overall sample preparation time.

The optimized method was then applied in triplicate to samples collected at different locations within the FDNPP near field, 14 bulk soils and 7 sequential extraction fractions, and the ^{137}Cs and ^{135}Cs activity concentrations and isotopic ratios were determined by QQQ-ICP-MS. The method resulted in LOD and LOQ for ^{133}Cs , ^{135}Cs and ^{137}Cs in the low pg/L range. The ^{137}Cs activity concentration in the soils varied among samples and as expected, ^{135}Cs activity levels were significantly lower but followed the same trend as ^{137}Cs . The measured $^{135}\text{Cs}/^{137}\text{Cs}$ isotopic ratios were similar to those reported in the literature, confirming the radiocesium contamination originated from the fallout during the FDNPP accident. However, there was no clear relationship between isotopic ratios and distance or direction from the FDNPP and thus could not be connected to the plumes released from the different reactor units. Finally, the sequential extraction samples showed similar isotopic ratio to the corresponding bulk samples, suggesting that the isotopic ratio did not change between the fractions Cs was bound to in the soils. Overall, this optimized method proved to be suitable for determining ^{135}Cs and ^{137}Cs in environmental complex samples by QQQ-ICP-MS analysis following microwave acid digestion and a simplified radiochemical separation using AMP and a cation exchange resin.

Sammendrag

Ulykken ved Fukushima Daiichi kjernekraftverk som skjedde i Japan 11. mars 2011 forårsaket radioaktivt utslipp, inkludert radioaktivt cesium (Cs). Dette utslippet kontaminerte områder nær anlegget samt store områder 50-70 km fra reaktorene. Målet med denne studien var å optimalisere publiserte metoder for radiokjemisk separasjon av radiocesium fra miljøprøver og måling av ^{137}Cs og ^{135}Cs ved trippelkvadrupol induktivt koplet plasma massespektrometri (QQQ-ICP-MS). Den optimaliserte metoden ville bli brukt til å bestemme isotopratio til $^{135}\text{Cs}/^{137}\text{Cs}$ for kildeidentifisering.

Metoden ble optimalisert ved testing og evaluering av tre forskjellige steg i prosedyren. En simulert løsning som inneholdt radiocesium, ble først evaluert til: i) tre separasjonsteknikker for Cs med AMP basert på gjenvinning av Cs og vanskelighetsgrad av jobben, og ii) anion- og kationresin basert på evnen til å fjerne uønskede ioner fra løsningen. To syreblandinger ble brukt på jordprøver i bulk fra Fukushima for å teste ekstraksjonskapasiteten til nedbrytning i mikrobølgeovn. Prøvene som inneholdt ^{137}Cs ble deretter målt på QQQ-ICP-MS for å sjekke gjenvinning av Cs og dekontamineringsfaktoren (DF) av uønskede ioner. Målingene viste at den optimaliserte metoden, som brukte konsentrert HNO_3 , 1 mg/mL AMP og 0.45 μm sprøytefilter, resulterte i ca. 75% og 100% gjenvinning av CS henholdsvis til nedbrytnings- og radiokjemisk separasjonstrinn. Basert på høye DF verdier for ioner som skaper interferens i ICP-MS, ble trinnet med anionresin fjernet, og dermed reduserte den totale prøveforberedelsestiden.

Den optimaliserte metoden ble deretter brukt i triplikater på prøver som ble hentet på forskjellige steder innenfor området til FDNPP, 14 jordprøver i bulk og 7 sekvensielle ekstraksjonsfraksjoner, og aktivitetskonsentrasjonen og isotopratioen til ^{137}Cs og ^{135}Cs ble bestemt med QQQ-ICP-MS. Metoden resulterte i lave deteksjons- og kvantifiseringsgrenser for ^{133}Cs , ^{135}Cs og ^{137}Cs i det lave pg/L området. Aktivitetskonsentrasjonen til ^{137}Cs i jordprøvene varierte mellom prøvene, og som forventet var aktivitetskonsentrasjonen til ^{135}Cs betydelig lavere, men fulgte samme trend som ^{137}Cs . De målte isotopratioene til $^{135}\text{Cs}/^{137}\text{Cs}$ var lik de tilsvarende verdiene fra litteraturen, som bekreftet at radiocesiumkontamineringen stammet fra nedfallet etter FDNPP-ulykken. Derimot var det ingen klar sammenheng mellom isotopratio og avstand eller retning fra FDNPP-området, og kunne derfor ikke kobles til nedfallet fra de forskjellige reaktorene. Til slutt viser de sekvensielle ekstraksjonsprøvene lignende isotopforhold til sine korresponderende jordprøver i bulk, som tyder på at isotopratioen ikke ble endret av hvilken fraksjon Cs var bundet til i jordprøvene. Totalt sett er den optimaliserte metoden egnet til å bestemme ^{135}Cs og ^{137}Cs aktivitetskonsentrasjon i komplisert sammensatte miljøprøver med QQQ-ICP-MS etter mikrobølge nedbrytning og en forenklet radiokjemisk separasjon med AMP og kationresin.

Table of contents

Acknowledgements.....	ii
Abstract.....	iii
Sammendrag.....	iv
Table of contents	v
List of Figures	vii
List of Tables	ix
1. Introduction	1
1.1 The Fukushima Daiichi nuclear power plant accident	1
1.1.1 The accident	1
1.1.2 Radionuclide release, dispersion, and deposition during the accident.....	1
1.2 Cesium.....	3
1.2.1 General chemical properties	3
1.2.2 Isotopes of cesium.....	3
1.2.3 Measurement of cesium isotopes	4
1.3 Radiochemical separations.....	5
1.4 Mass spectrometry (MS)	6
1.4.1 Inductively plasma coupled mass spectrometry (ICP-MS).....	6
1.4.2 Interferences in mass spectrometry.....	9
1.4.3 Determination of radiocesium by mass spectrometry	10
1.5 Aim and objectives of the thesis	11
2. Materials and methods	12
2.1 Reagents and solutions	12
2.2 General protocols and instrument settings	12
2.2.1 Microwave acid digestion.....	12
2.2.2 Gamma spectrometry	13
2.2.3 Inductively coupled plasma – optical emission spectrometry (ICP-OES)	13
2.2.4 Inductively coupled plasma – mass spectrometry (ICP-MS)	15
2.3 Radiochemical separation optimization	16

2.3.1 Step 1: AMP sorption + separation.....	16
2.3.2 Steps 2 and 3: Anion and cation exchange resins.....	19
2.3.3 Decontamination factor and recovery.....	20
2.4 Optimization of soil digestion.....	21
2.4.1 Acid mix digestion test	21
2.4.2 Re-testing step 2 – anion exchange resin	22
2.5 Fukushima samples	22
2.5.1 Sample details	22
2.5.2 ¹³⁵ Cs/ ¹³⁷ Cs isotope ratio measurements.....	25
3. Results & discussion	26
3.1 Method optimization	26
3.1.1 Evaluating the matrix	26
3.1.2 Removing interfering ions	29
3.1.3 Digestion optimization	35
3.1.4 Digestion and radiochemical separation optimization	37
3.1.5 The optimized method	39
3.2 Isotopic ratio in Fukushima soil samples	40
3.2.1 Activity concentration of radiocesium.....	40
3.2.2 ¹³⁵ Cs/ ¹³⁷ Cs isotopic ratio in contaminated soils from Fukushima exclusion zone	47
4. Conclusions and further research	52
References	54
Appendix.....	57

List of Figures

Figure 1. 1: Aerial measurements from the northwestern fallout of the Fukushima accident. The different sub-pictures show different dates after the accident, ranging from April 29 th , 2011, on the top-left to November 7 th , 2014, on the bottom-right. The dose measured is in $\mu\text{S/h}$ (IAEA, 2015; NRA, 2015).	2
Figure 1. 2: Isotopic ratio of $^{135}\text{Cs}/^{137}\text{Cs}$ from Fukushima environmental samples (blue), damaged reactor cores (orange) and spent fuel rods (green) (Zheng et al., 2014b).	4
Figure 1. 3: Illustration of the process of MS with quadrupoles for ^{137}Cs and ^{137}Ba using N_2O and NH_3 as reaction gas.	9
Figure 2. 1: Step 1 of the radiochemical separation comprising the sorption of Cs on AMP, separation from the solution and dissolution of the AMP.	17
Figure 2. 2: Steps 2 and 3 of radiochemical separation including anion and cation exchange resin in columns to purify sample containing Cs.	19
Figure 3. 1: Concentrations of Cs and Ba (in $\mu\text{g/L}$) in the simulated solution after steps 1, 2 and 3 of the radiochemical separation (A) and after steps 1 and 2 only (B), using 3 different types of separation in step 1 (paper filter, centrifugation, and syringe + filter) and 3 different concentrations of AMP (1, 5 and 10 mg/mL). Error bars represent the standard deviation of duplicate samples (* = one replicate). Note the different scale for Ba concentrations in A for samples after steps 1 and 2.	30
Figure 3. 2: Recovery of ^{133}Cs (in %) in simulated solution after 3 steps of the radiochemical separation (A) and after step 1 and step 2 only (B), using 3 different types of separation in step 1 (paper filter, centrifugation, and syringe + filter) and 3 different concentrations of AMP ranging from 1 to 10 mg/mL . Error bars represent the standard deviation of duplicate samples (* = one replicate).	31
Figure 3. 3: Decontamination factor of Ba in simulated solution after 3 steps (A) and after step 1 and 2 only (B) of the radiochemical separation, using 3 different types of separation in step 1 (paper filter, centrifugation, and syringe + filter) and 3 different concentrations of AMP ranging from 1 to 10 mg/m L . Error bars represent the standard deviation of duplicate samples (* = one sample).	31
Figure 3. 4: Photo of soil samples after acid microwave digestion: (A) with acid mix 1 (only HNO_3) and (B) with acid mix 2 (HNO_3 , H_3PO_4 and HBF_4). The dark solids in the bottom of tubes in (A) are undigested sample materials.....	37

Figure 3. 5: The optimized method for measuring ^{135}Cs in complex soil matrixes by QQQ-ICP. . 40

Figure 3. 6: Average activity concentration in Bq/g of ^{137}Cs in digested bulk samples versus the distance from the FDNPP reactors to the sampling sites. Error bars represent 1 standard deviation of triplicate samples. Number on top of bars indicate sampling site. Measured by QQQ-ICP-MS. 42

Figure 3. 7: Average ^{137}Cs (A) and ^{135}Cs (B) activity concentration (in Bq/g) for Fukushima bulk and sequential extraction triplicate soil samples after radiochemical separation without step 2, measured by ICP-MS. Sample labels indicate sampling location within the Fukushima exclusion zone (Table 2.3). Error bars represent 1 standard deviation of triplicate samples..... 46

Figure 3. 8: Average isotopic ratio of $^{135}\text{Cs}/^{137}\text{Cs}$ measured in bulk soil samples as a function of distance of the sampling site from the reactor. Color code indicates the direction of the sampling site respect to the reactor (i.e., WSW = west-south-west, WNW = west-northwest, SSE = south-south-east and SSW = south-south-west). Error bars represent 1 standard deviation of 5-7 replicate measurements on 3 replicate samples..... 49

Figure 3. 9: Overview map of the Fukushima landscape including the sampling site locations with the corresponding isotopic ratios of bulk soils (Table 3.3). Color boxes indicate the site direction with respect to the FDNPP reactors. Details of sampling sites and sample characteristics can be found in Table 2.3. 50

Figure 3. 10: Average isotopic ratio of $^{135}\text{Cs}/^{137}\text{Cs}$ of sequential extraction samples. Labels indicate from the sampling location within the Fukushima exclusion zone (Table 2.3). Error bars represent 1 standard deviation of 5-7 replicate measurements on 3 replicate samples. 51

List of Tables

Table 2. 1: General instrument settings for ICP-OES analyses.	14
Table 2. 2: General instrument settings for ICP-MS analysis using S-lens.	16
Table 2. 3: Sample details for Fukushima soil samples. Samples were collected by NMBU staff on field trip to Fukushima in September 2016 (Reinoso-Maset et al., 2020). Details include distance to reactor from sampling site, wind direction, general depiction of sample site, type of sample, depth of collection and the organic content. The sequential extraction samples (step 6, 7 M HNO ₃) were obtained by Tetteh, 2018. Original label names are shown together with the correspondence to the bulk sample numbers in brackets.	24
Table 3. 1: Concentrations and decontamination factors (DF) for Al, Ba, Ca, K, Mg, Mo and Na measured by ICP-OES in simulated solution samples after the full radiochemical separation procedure and after step 2. Sample names indicate step 1 separation method (i.e., paper filter, centrifuge, syringe) and amount of AMP (i.e., 1, 5 or 10 mg/mL). Reported DF values are based on measured concentrations or the ratio of the method's detection and quantification limits (LOD/LOQ; based on method blanks) for each element.	27
Table 3. 2: Concentrations (and 1 standard deviation) of elements of interest to evaluate step 2 when using soil samples. Three replicates of a soil sample underwent the full radiochemical separation (Step 1+2+3) and 3 replicates underwent the radiochemical separation without step 2 (No step 2).....	38
Table 3. 3: Results for Fukushima bulk and sequential extraction soil samples. Sampling sites details (distance and wind direction) and average activity concentration of ¹³⁵ Cs and ¹³⁷ Cs as well as the average isotopic ratio of ¹³⁵ Cs/ ¹³⁷ Cs with standard deviation and RSD are reported. All data for ¹³⁵ Cs and ¹³⁷ Cs were decay-corrected back to date of accident and corrected for loss in digestion.....	43

1. Introduction

1.1 The Fukushima Daiichi nuclear power plant accident

1.1.1 The accident

The accident at the Fukushima Daiichi nuclear power plant (FDNPP) happened the 11th of March of 2011. According to reports from the United Nations Scientific Committee on the Effects of Atomic Radiation and the International Atomic Energy Agency (UNSCEAR, 2014) (UNSCEAR, 2014) (IAEA, D. G., 2015), a devastating earthquake of a 9.0 magnitude, called The Great East Japan Earthquake, happened near Honshu island, Japan. A 500 km x 200 km of the crust of the earth burst, creating a tsunami with waves reaching over 10 m in height (IAEA, D. G., 2015). The results of the earthquake were destruction and flooding of property and land, as well as over 20,000 lives were lost (UNSCEAR, 2014). Another result of the earthquake was damage to three of the six nuclear reactors at the FDNPP site, which according to the UNSCEAR report resulted in the worst civil nuclear disaster since Chernobyl in 1986. The IAEA and UNSCEAR reports stated that the electricity both off- and on-site caused failure to the power plant safety, operation, and cooling systems, which led to severe core damage to the three reactors, unit 1-3. Unit 4 also suffered damage but was shut down along with unit 5-6 for maintenance. The other power plants in Japan were safely shut down.

1.1.2 Radionuclide release, dispersion, and deposition during the accident

The disaster led to the release of radioactive material into the environment for a prolonged amount of time. The wind at that time caused most of the atmospheric release to travel eastwards into the Pacific Ocean, while only a small portion of the release deposited on land in a north-western direction from FDNPP (IAEA, D. G., 2015). In the immediate aftermath of the accident, plumes with noble gases such as ⁸⁵Kr and ¹³³Xe, including isotopes ¹³¹I, ¹³⁴Cs and ¹³⁷Cs, as well as radioactive nuclides of strontium, ruthenium and actinides were released (IAEA, D. G., 2015). The atmospheric release consisted mostly of the noble gases, where it is estimated a release of 6000-12000 PBq of ¹³³Xe, while the release of ¹³¹I and ¹³⁷Cs were substantially lower, with rates of 100-400 PBq and 7-20 PBq respectively. (IAEA, D. G., 2015). As most of the radioactive release blew eastwards, a great deal of the radiation dispersed into the Pacific

Ocean. That said, some of the release went inwards land because the wind changed direction. This caused the deposition of radionuclides on land mostly in a north-west direction from FDNPP. The total release from the Fukushima accident was estimated to be 900 PBq, compared to the Chernobyl accident which had estimated release of 5200 PBq (Choppin et al., 2013). The total amount of ^{137}Cs deposition from the accident were estimated to be around 2-3 PBq on land. Since Cs can move easily through the environment and under the effects of weathering, the Cs dispersed, and the density of the deposition decreased (IAEA, D. G., 2015). Researchers studied deposition in Hibara lake 100 km away from FDNPP. The team detected ^{134}Cs and ^{137}Cs in all sediments of the shallow area of the lake, where silt and clay had most of the Cs-fraction at the peak level between 0-5 cm (Basuki et al., 2018). They also reported that the indirect deposition in steep areas came from erosion and rainfall, while flatter areas relied on flowing sediments from rivers. Figure 1.1 presents the ambient dose on terrestrial land over the period from 29th of April 2011 to 7th of November 2014.

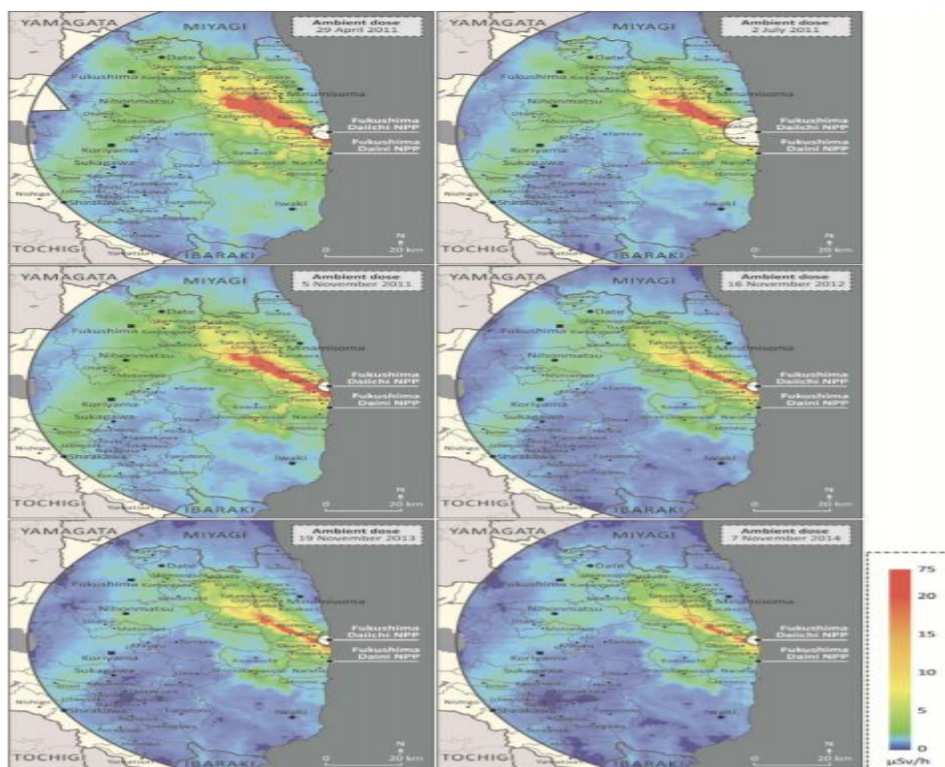


Figure 1. 1: Aerial measurements from the northwestern fallout of the Fukushima accident. The different sub-pictures show different dates after the accident, ranging from April 29th, 2011, on the top-left to November 7th, 2014, on the bottom-right. The dose measured is in $\mu\text{S}/\text{h}$ (IAEA, 2015; NRA, 2015).

1.2 Cesium

1.2.1 General chemical properties

Cesium (Cs) is an element with the atomic number 55. It was discovered in 1860 by R. Bunsen and G. Kirchoff, and Cs is the rarest naturally occurring alkali metal (Gad & Pham, 2014). Cesium is found in low amounts with other elements in rocks, soil and dust (NCBI, 2021). Visually a silver-white soft element, and the natural resonance frequency of excited cesium atoms is used to make atomic clocks (Aronson, 2016). Cesium has 40 isotopes ranging from 112 to 151 in atomic mass (Andersen, 2016), with ^{133}Cs as the only stable isotope. The most mentioned isotopes are ^{134}Cs and ^{137}Cs , which are a product of nuclear fission from nuclear power plant fuel rods with ^{235}U , nuclear reactor explosions and weapons. The ^{137}Cs isotope causes major problems for the environment because of its effect on agriculture and stock farming combined with relative long half-life (Yasunari et al., 2011).

1.2.2 Isotopes of cesium

Every source of anthropogenic Cs-pollution has a fingerprint which can be found through the ratios of the different species. The ratio between $^{135}\text{Cs}/^{137}\text{Cs}$ has been commonly used as a tracer to finding pollution sources regarding FDNPP (Zheng et al., 2014a). Figure 1.2 shows the isotopic ratio of $^{135}\text{Cs}/^{137}\text{Cs}$ from environmental samples, damaged reactor cores and spent fuel pools from the Fukushima area after the accident in 2011. The difference occurs in the specific reactors, which uses fuel and burn differently, which will affect the ratios (Chino et al., 2016). The problem with this ratio is the half-lives of the isotopes, where ^{137}Cs has a half-life $t_{1/2} = 30.02$ years, while ^{134}Cs only has a half-life of $t_{1/2} = 2.065$ years (IAEA, 2021). That means that the source of ^{134}Cs will be considered dead in 20 years after the accident because of its short half-life, as it will pass 10 times half-life. This is a problem, and newer methods of analyzing Cs-pollution need to be found to continue the environmental research. Therefore, the $^{135}\text{Cs}/^{137}\text{Cs}$ ratio has been introduced by many research groups (Russell et al., 2014; Zheng et al., 2014a; Zheng et al., 2014b; Zheng et al., 2016), as the half-life of ^{135}Cs is substantially longer with $t_{1/2} = 2.3 \cdot 10^6$ years (IAEA, 2021). This ratio also works as a fingerprint for determining the source of Cs-pollution. Cesium-135 is shielded from $^{135}\text{Xe} - ^{136}\text{Xe}$ during neutron capture in fission chains,

while ^{137}Cs remains unaffected, which means that the ratio will be characteristic for different types of reactors (Zheng et al., 2014a).

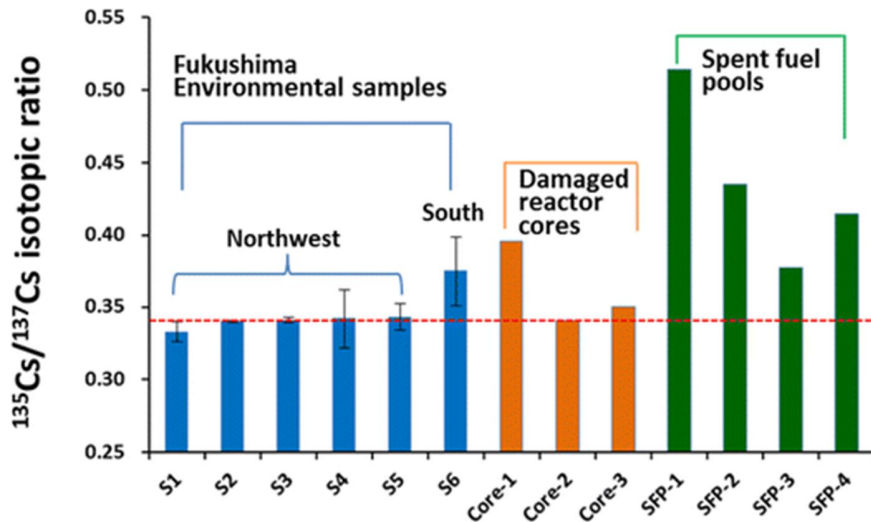


Figure 1. 2: Isotopic ratio of $^{135}\text{Cs}/^{137}\text{Cs}$ from Fukushima environmental samples (blue), damaged reactor cores (orange) and spent fuel rods (green) (Zheng et al., 2014b).

1.2.3 Measurement of cesium isotopes

Radiocesium can be measured by different techniques. For example, fluorescence quenching can be used to detect Cs metal ions in aqueous solutions by absorbance (Radaram et al., 2013). This method uses the properties of light, where an excited atom will release its energy and emit light, called fluorescence, presents low detection limits and high sensitivity towards Cs, and is non-destructive and cheaper compared to other methods such as mass or gamma spectrometry.

The most common radiometric technique to measure ^{137}Cs is gamma spectrometry. Gamma counters, such as NaI-detectors, are commonly used. The instrument consists of a cylindrical NaI-crystal connected to a photo-multiplier tube and registers the energy from gamma rays that is released by radionuclides. The peak energy for ^{137}Cs is 661.7 keV. As radioactive decay is stochastic, counting time will improve the statistics for the measurement.

Mass spectrometry can also be used to measure ^{137}Cs . This analytical technique has the advantage of low detection limits, reduced measuring time, minimal matrix effect and measurement of isotopic ratios; however, it is a destructive technique, requires the ions in

aqueous form, and has higher running costs than other basic analytical techniques. Moreover, samples must often go through a radiochemical separation to remove most of the matrix. On the other hand, the use of quadrupoles in QQQ-ICP-MS can remove ions with unwanted mass, giving low interference from isobaric isotopes and polyatomic compounds.

1.3 Radiochemical separations

Radiochemical separation is a technique used to prepare radioactive samples for analysis. Different samples have different matrices that can include elements that can interfere with the analysis. It is therefore important to separate the wanted radionuclides from unwanted interferences to be able to perform measurements accurately.

In order to carry out radiochemical separations, it is important to know as much as possible about the sample characteristics and in what state the radionuclides exist in. This knowledge helps with making the decision on what radiochemical separation to perform, as there are different methods. The most common methods are solvent extraction, ion exchange chromatography and extraction chromatography (Reinoso-Maset, 2020). The solvent extraction method, also called liquid-liquid extraction (LLE), is based on the solubility of the analyte in two liquids that do not mix and will separate into layers (Reinoso-Maset, 2020). The components in the method can vary and different liquids can be used to extract the analyte. Although that is good, the process of separation is tedious, as the method may require several extractions to obtain most of the analyte.

The ion exchange chromatography separation uses resins to absorb either the analyte or interfering cations or anions in the solution. The method often involves use of acids to vary the pH level of the solution to elute either the analyte or interfering cations and anions. Since the resin must have the appropriate properties to efficiently separate the wanted radionuclide, there are different resins for different radionuclides. The method itself can be slow but has the advantage of the possibility to run multiple samples simultaneously. Extraction chromatography involves a packed column with three phases present: the stationary phase, the mobile phase, and the inert support. The inert phase is made of porous material, often silica or polymers, whereas the stationary phase is made of ionophores immobilized on the inert phase (Reinoso-

Maset, 2020). Different and multiple kinds of resins are used depending on the properties of the analyte. When the sample goes through the column in the mobile phase it will have different retention times depending on the affinity between analyte(s) and stationary phase. That will cause different elements to elute from the column at different times. Knowing this and the properties of the analyte and resins used, the analyte can be eluted alone.

1.4 Mass spectrometry (MS)

In mass spectrometry (MS), differences in atomic weight makes it possible to separate, analyze and quantify different elements (Equation 1).

(Equation 1)
$$\text{Mass-to-charge ratio} = m / z$$

where m is the mass and z is the charge of the ion or molecule analyzed. For example, atoms with a charge of $z = 1$ will have a mass-to-charge ratio of its atomic weight, as it is divided by 1, whereas atoms with a charge of $z = 2$ will have their ratio divided by 2 and could interfere with other atoms or molecules with the same mass-to-charge ratio.

Mass spectrometry has four essential steps: ionization of analyte, separation of mass, detection of wanted masses, and analysis of the result. Ionization of the analyte can happen by different means, for example, by inductively coupled plasma (ICP), electrospray ionization (ESI) and thermal ionization (TI). The other three steps happen in the MS-part of the instrument (see section 1.4.1).

1.4.1 Inductively plasma coupled mass spectrometry (ICP-MS)

When using an ICP-MS Triple Quad (Agilent Technologies), the injected sample will first pass through a loop using a peristaltic pump. It is important to have enough volume in the loop to get enough supply of sample. The peristaltic pump makes it possible to control the fluid flow as well as to ensure that it is constant and as pulse-free as possible. From the loop, the sample passes through a nebulizer, which is an apparatus that converts the sample solution into a mist of small aerosols. The most common ones are the concentric, cross-flow and Babington nebulizers, and the use depends on the properties of what is being analyzed (*The 30-Minute Guide to ICP-MS*, 2004). The mist from the nebulizer enters a spray chamber, most commonly a

Scott or cyclonic spray chamber (*The 30-Minute Guide to ICP-MS*, 2004). The largest droplets travel to the side, while droplets smaller than 10 µm pass through to the plasma. This is important, as larger droplets can interfere with plasma and make it unstable and colder. From the spray chamber, the sample will enter the plasma, which is the ionization source of the instrument.

To generate plasma, a radio frequency signal coil is used to generate a magnetic radio frequency field. The energy this field creates is the origin of the energy of the plasma. Ions and electrons that are formed will achieve high kinetic energy by interaction with the magnetic field, which creates friction. Argon (Ar) gas of several liters per minute is emitted from a torch and will form plasma by chain reaction of collisions, where argon atoms are ionized by colliding with other argon atoms, as shown in equation 2. However, only about 5% of all argon atoms are ionized.



The chain reaction of collisions causes the plasma to reach very high temperatures and has an operating temperature of about 7500 K and higher. Since the temperature is so high, the torch, which is made of three concentric quartz tubes, must be cooled down. This is also done by argon gas in the outer tube going through the torch.

The sample is introduced into the plasma through the central narrow tube in the torch. The elements ionize to a greater or lesser degree, depending on the ionization energy of the element. Elements with high ionization energy will be more ionized than elements with lower ionization energy. The sample will also dry up and heated into gas because of the high temperature in the plasma. From plasma, the elements pass through two cones, called sampler and skimmer cones. These are two rings with small orifices in the middle that extract ions from the plasma. Since these cones, often made of nickel or platinum, are located right next to the plasma, they are cooled with water to prevent melting. The pressure difference here is vast, and the instrument needs vacuum pumps to drop the pressure inside and after the cones. Furthermore, the sample with analyte passes through the last cone and onto the ion lenses that are positively and negatively charged. This means that the path to the analyte is bent off and

will not be in axis with the plasma. This ensures that photons, neutrals, and electrons do not pass further into the detector. This vacuum ensures that the air in the system is removed. This is done because there are unwanted atoms and molecules in the air, which can interfere with the ions in the event of a collision. The ion lenses also form an ion beam, as non-ionized atoms will be separated.

The positive ion current proceeds to the separation of mass, which happens in the quadrupoles. A quadrupole consists of four parallel electric rods. These rods are divided into opposing pairs, which ensure that the ions stay within the path of the quadrupole. The rods are fitted with direct current and alternating current which forms an electromagnetic field between the paired, parallel rods. The ion pathways are very important to be able to separate by mass. By changing conditions such as voltage and frequency, only the desired mass will pass through the path. Other masses will not be able to follow the path and will collide and fall away.

Agilent 8800 is a triple quadrupole, which means that it contains two quadrupoles and a reaction-collision cell, called an octupole. A simple illustration of this is presented in Figure 1.3. A reaction-collision cell is included between the quadrupoles to remove interferences. This can be done by reacting the analyte with a gas to change the mass. An example of this is arsenic (As), which has a mass of 75 u. By reacting arsenic with oxygen, arsenic oxide is created, which has a mass of 91 u. By setting the next quadrupole of 91 u, only AsO will go through the second quadrupole. The reaction-collision cell can also be used to collide with, e.g., polyatomic compounds. The gas in the cell will collide with the atoms, which lose kinetic energy. At the end of the reaction-collision cell there is a voltage field with an energy barrier. If the atom does not have enough kinetic energy, it will not be able to pass through. Thus, the reaction-collision cell works well to remove interferences.

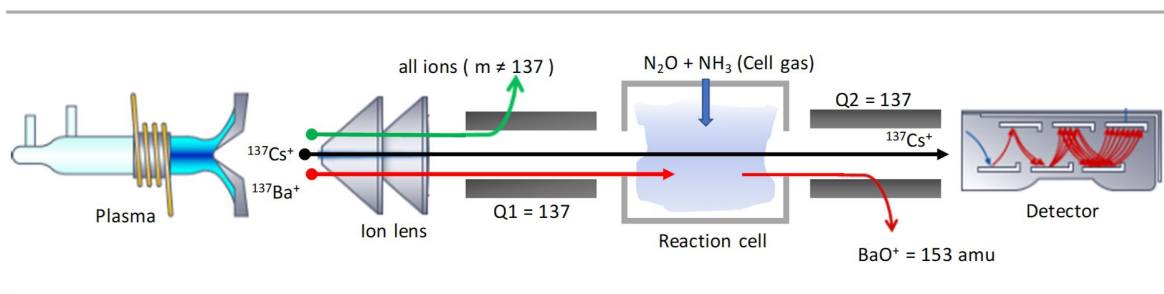


Figure 1. 3: Illustration of the process of MS with quadrupoles for ^{137}Cs and ^{137}Ba using N_2O and NH_3 as reaction gas.

After the analyte has passed through the quadrupole system, it will reach the detector. In the Agilent 8800, the detector consists of an electron multiplier with 20 dynodes. The analyte coming to the detector will release electrons from the first dynode, which is negatively charged. Furthermore, these electrons will move on to a positive dynode, which will release new electrons. This happens in up to 20 dynodes, which amplifies the signal. This signal can be measured in two different ways. Either as the number of pulsations or the number of counts per second. This detector is used at low concentrations. If the concentration is too high, the current can be measured and converted to the number of counts per second. The instrument comes with software on a computer. The software is updated with interferences and can also correct for spectral interferences between isobaric atoms.

1.4.2 Interferences in mass spectrometry

ICP-MS is an analytical technique known to have few interferences. A couple of these are mentioned earlier, with isobaric atoms or double-charged atoms. Isobaric atoms are atoms of different elements, but with the same mass. The isotope ratio of an element is well known. Thus, other isotopes from the interfering element can be measured. This makes it possible to subtract the signal from the interference from the analyte.

Since only 5% of the argon atoms are ionized, Ar has a relatively high initial ionization energy, higher than the first ionization energy for most other elements. However, this does not apply to all elements which can be double charged, which causes the mass-to-charge ratio to change. For example, double-charged atoms can be a problem for, among others, As. Samarium-150 tends to be double-charged and will pass through the quadrupoles with the same mass-to-

charge ratio as As. A solution is to use oxygen in the reaction-collision cell to react As^+ to form AsO^+ so that the mass has changed too and the mass-to-charge ratio is different than $^{150}\text{Sm}^{2+}$.

Polyatomic compounds can be formed in the cold part of plasma or by reaction with gas in the reaction-collision cell. The gas in the reaction-collision cell can also collide with these compounds. Thus, the choice of gas, or no gas, is an important part of the method. In addition, analytes with high mass numbers and high concentrations can cause a sensitivity drop for the lighter elements. This effect is called space charge effects.

Complex sample matrices can cause problems for the analysis. For example, seawater contains salts that can clog the cones as well as other elements that can interfere with the analyte. If the sample is well diluted, this problem can be avoided.

With long analyzing runs, maintaining the initial instrument operation can become challenging as measuring conditions can change throughout the analysis. For example, calcium can build-up on the cone. These changing conditions can be corrected for by using an internal standard. The internal standard should have the same chemistry and mass as the analytes in the sample, so that if the signal to the internal standard varies, the signals of other elements equally change. This can be used to correct for operation, which threshold is usually set to $\pm 2.5\%$. Moreover, background equivalent correction (BEC) can be used to correct for background signal. BEC is calculated from counts of the blank in the standard calibration curve.

1.4.3 Determination of radiocesium by mass spectrometry

Measuring ^{135}Cs is harder by radiometric techniques than ^{137}Cs because of its long half-life and low-energy beta-decay (Zheng et al., 2014a). Moreover, mass spectrometry techniques such as TIMS, neutron activation analysis (NAA) and accelerator mass spectrometry (AMS) are unsuitable techniques due to their limited availability and cost (Zheng et al., 2014a). Therefore, new methods with QQQ-ICP-MS as the instrument is on the rise. The advantage of this method is the removal of isobaric, mostly with barium, and polyatomic interferences with molybdenum, tin and antimony (Zheng et al., 2016) using a collision cell with nitrous oxide gas (N_2O gas) following a separation with ammonium molybdophosphate (AMP) and ion exchange chromatography. AMP is highly selective towards Cs atoms and can separate Cs from seawater,

sediment, soil, spent fuel, etc. (Russell et al., 2014). This step is often followed by an anion- and cation-exchange chromatography to separate Cs from the matrix (Zheng et al., 2016). These separation methods work great on samples of smaller size but will struggle on larger samples sizes due to alkali and alkaline metals like K and Ca which exists in the matrix (Zheng et al., 2016). These metals can decrease Cs ionization because of formation of salt on cones in the ICP-MS, resulting in lower signal (Zheng et al., 2016). If this remains the case, a method that removes Cs from the matrix more effectively is needed. For example, using AMP followed by a two-stage ion-exchange chromatography can effectively remove major interfering agents such as alkali and alkaline metals alongside isobaric and polyatomic interferences, which in turn result in a reliable analysis with very low detection limits for ^{137}Cs and ^{137}Cs (Zheng et al., 2016).

1.5 Aim and objectives of the thesis

The overall aim of the thesis was to develop a standardized procedure for measuring the activity concentration and isotopic ratio of $^{135}\text{Cs}/^{137}\text{Cs}$ in complex environmental samples, which will allow to lower cost and analysis time of an experiment. The method development was focused on in-depth examination of every step of the procedure from sample to measurement by QQQ-ICP-MS. This study was divided into three specific objectives:

1. To optimize a published methodology utilizing AMP followed by cation and anion resins for optimal radiochemical separation of ^{135}Cs . Every step of the radiochemical separation had to be evaluated and optimized based on the following factors: recovery of analyte, necessity of steps for interferences minimization, time at each step, and conveniency to work with.
2. To measure the isotopic ratio of $^{135}\text{Cs}/^{137}\text{Cs}$ by QQQ-ICP-MS after applying the optimized radiochemical separation method. In order to obtain accurate results for the $^{135}\text{Cs}/^{137}\text{Cs}$ isotopic ratio, the QQQ-ICP-MS method was optimized to obtain low detection and quantification limits for ^{135}Cs and ^{137}Cs and acceptable rates of interference from isobaric and polyatomic ions originated from the matrix.
3. To accurately measure the $^{135}\text{Cs}/^{137}\text{Cs}$ isotopic ratio in Fukushima soils samples and deduce the source of the radiocesium contamination. The results will be checked against other studies reporting the $^{135}\text{Cs}/^{137}\text{Cs}$ isotopic ratios of environmental samples from the FDNPP area.

2. Materials and methods

2.1 Reagents and solutions

High purity water (18.0-18.3 M Ω cm⁻¹), referred hereafter as MilliQ water, was used to prepare all solutions in this work. MilliQ water was obtained by passing grade II water (NS EN ISO3696, MilliPore RiOs 50) through a 2 housing B-pure water purification system (Barnstead, USA). Nitric acid (HNO₃) 65% (AnalaR NORMAPUR from VWR Chemicals) was used in the preparation of standard solutions, simulated samples, and diluted samples for analysis (5% V/V) as well as in the radiochemical separation steps and digestion of soil samples. Hydrochloric acid (HCl) 37% (AnalaR NORMAPUR from VWR Chemicals) and ammonium hydroxide (NH₄OH) 30% (Sigma-Aldrich) were used to prepared diluted solutions used in the different radiochemical separation steps. Fluoroboric acid (HBF₄) 48% (Sigma-Aldrich) and phosphoric acid (H₃PO₄) 85% (Bio-Ultra), were used in digestion of soil samples. Ammonium molybdophosphate hydrate (AMP) powder purchase from Sigma Aldrich was used in the radiochemical separation method.

A simulated solution was prepared in 200 mL batches in 5% HNO₃ (V/V) using 100 mL of the 1643H house standard, which contains the following elements: Al, Sb, As, Ba, Be, B, Cd, Ca, Cr, Co, Cu, Fe, Li, Mg, Mn, Mo, Ni, P, Ru, Se, Ag, Na, Sr, Te, Tl, V, Zn, U, Th, S, Si, Cs, La, Ce, Pr, Nd, Sm, Eu, Gd, Dy, Ho, Er, Tm, Yb, Lu, Zr, Nb, Ga. The concentrations of Cs, Ba and Al were increased by adding 0.2 mL of 0.01 g/L, 2 mL of 10 g/L and 1 mL of 1 g/L ICP standard solutions (Inorganic Ventures, USA) respectively. The final concentrations are shown in Appendix 1. Standard solutions for ICP-OES and ICP-MS analyses were all made from ICP standard stock solutions (1-10 g/L, Inorganic Ventures) in 5% HNO₃ V/V.

2.2 General protocols and instrument settings

2.2.1 Microwave acid digestion

Soil samples were fully digested using a microwave assisted digestion system (UltraWave ECR, Milestone). Dried soil samples, ca. 0.5 g, were added to acid-cleaned Teflon tubes followed by 5 to 10 mL of concentrated acid. Depending on which acid mix was used, samples were stirred on a tube shaker for 10 to 20 seconds. Blank samples contained only concentrated acid at the same volume as the samples. The Teflon tubes were corked and loaded into the UltraWave. The

samples were digested for 40 minutes at 260 °C with 10 minutes warmup and 15 minutes cooldown. After digestion, the contents of the Teflon tubes were transferred to 15 mL centrifuge tubes by decanting. Each Teflon tube was rinsed 3 times with MilliQ water. Rinse water was added to each respective 15 mL centrifuge tube until just under 15 mL of volume. The centrifuge tubes were filled up to the 15 mL mark with MilliQ water and left to sediment until the next day.

2.2.2 Gamma spectrometry

The total ^{137}Cs activity in soil and sequential extraction samples were determined by gamma spectrometry at 661.7 keV using a NaI-detector (Wizard 3" 1480 automatic gamma counter, Perkin Elmer Life Sciences) in LSC vials. The samples were counted for 10 to 20 minutes to provide good analytical precision and low counting uncertainty, especially for samples with low activity (< 2 Bq). Blank samples from radiochemical separation and/or digestion and empty vials were used as blank samples and always put as the first and last vials within the run. These blank samples were used to determine the limit of detection (LOD) and limit of quantification (LOQ) of ^{137}Cs of the gamma radiation measurements. Reference materials IAEA-300 and IAEA-373 (International Atomic Energy Agency, 1993 & 1996, appendix 2) were also measured to calculate the accuracy of the instrument. Activity concentrations (Bq/g) were calculated from the corrected counts per minute (CPM; calculated by removing the background activity) and given respect to the dry mass of the sample.

2.2.3 Inductively coupled plasma – optical emission spectrometry (ICP-OES)

Simulated solutions and aliquots collected from different steps of the radiochemical separation were measured on an Agilent 5110 ICP-OES to determine the decontamination factor of various elements. The general instrument settings are shown in Table 2.1. Standard solutions used were prepared from 1 mg/L (Ba), 10 mg/L (K, Mg, Mo, and Na) and 100 mg/L (Ca) ICP stock solutions (Inorganic Ventures) in 5% (V/V) HNO_3 . Samples were measured at 1 or 2 wavelengths for each of the elements. LOD and LOQ for the measured analytes were determined from 8 wash samples (instrumental LOD/LOQ) or 9 blank samples (method LOD/LOQ). Concentrations were dilution corrected and results (in mass concentration, $\mu\text{g/L}$ or mg/L) were obtained by the instrument's software.

Table 2. 1: General instrument settings for ICP-OES analyses.

Parameter	Settings
Type	Analyte
Background correction	Fitted
Number of pixels	2
Element and wavelength	Al, 167.019 nm, peak 167.015 nm
	Al, 396.152 nm, peak 396.145
	Ba, 455.403 nm, peak 455.399
	Ba, 493.408 nm, peak 493.397 nm
	Ca, 396.847 nm, peak 396.839
	Ca, 422.673 nm, peak 422.644 nm
	K, 766.491 nm, peak 766.491
	Mg, 279.553 nm, peak 279.548 nm
	Mg, 285.213 nm, peak 285.207 nm
	Mo, 202.032 nm
	Mo, 203.846 nm
	Mo, 204.598 nm
	Na, 589.592 nm
Replicates	3
Pump speed carrier	10 rpm
Pump rate - Uptake	23.0 mL/min
Pump rate - Inject	9.0 mL/min
Valve uptake delay	8.0 s
Bubble injection time	0.8 s
Preemptive rinse time	0.0 s
Rinse time	10.0 s
Read time	5.0 s
RF power	1.50 kW
Stabilization time	9.0 s
Viewing mode	Radial
Viewing height	2.0 mm
Nebulizer flow	0.70 L/min
Plasma flow	12.0 L/min
Aux flow	1.00 L/min
Makeup flow	0.00 L/min

2.2.4 Inductively coupled plasma – mass spectrometry (ICP-MS)

Soil and sequential extraction samples were measured on an Agilent 8900 #100 triple-quadrupole mass spectrometer (QQQ-ICP) to determine the activity concentration, recovery, and isotopic ratio of ^{135}Cs and ^{137}Cs and the recovery of ^{133}Cs . An Agilent 8800 QQQ-ICP was used to screen through most of the periodic table and evaluate high concentrations of various elements that could affect the measurements by ICP-MS when using the Apex Q nebulizer (Elemental Scientific, Omaha, Nebraska, USA). Standard solutions for ^{133}Cs were prepared from an ICP standard solution (10 mg/L; Inorganic ventures) in 5% (V/V) HNO_3 . A ^{137}Cs source stock solution was used to prepare ^{137}Cs standard solutions in 5% (V/V) HNO_3 (0.81 – 8.1 Bq/mL, 0.25 – 2.5 ng/L) on 11.01.2021. The ^{137}Cs source stock solution was prepared from an intermediate stock solution of 121.21 Bq/mL (4243 Bq ^{137}Cs in 50 mL) on 30.05.2018. The ^{137}Cs source solution was prepared with 1.1468 mL of 370 kBq ^{137}Cs as CsCl in 0.1 M HCl (10 μg Cs/mL) at a certified date of 01.09.2017. Standard solutions for screening with the Agilent 8800 QQQ-ICP-MS were prepared from a multi element standard (71A – D, Inorganic Ventures). Results (in mass concentration, $\mu\text{g/L}$ or mg/L) obtained by the instrument's software were dilution corrected. To determine the activity concentration of ^{137}Cs and ^{135}Cs in the soil samples (in Bq/g), the weighed dry mass of the samples was used. The recovery of ^{137}Cs was determined by comparing the concentration of ^{133}Cs before and after radiochemical separation. The general instrument settings can be found in Table 2.2.

Table 2. 2: General instrument settings for ICP-MS analysis using S-lens.

Parameter	Settings
Scan type	MS/MS
Monitored mass pairs (Q1 -> Q2)	115 -> 115 In 0.25 s
Integration time per mass	118 -> 118 Sn 0.20 s
* <i>Internal standard</i>	133 -> 133 Cs 0.25 s
	135 -> 135 Cs 7.00 s
	137 -> 137 Cs 7.00 s
	137 -> 188 Ba 0.25 s
Replicates and sweeps	7 replicates, 150 sweeps per replicate
RF Power	1600 W
Sample depth plasma	7.0 mm
Nebulizer gas flow	0.83 L/min
Spray chamber temperature	2.0 °C
Makeup gas flow	0.30 L/min
<i>Collision-reaction cell</i>	
He Flow rate	1.0 %, 1.0 mL/min
H ₂ Flow rate	OFF
NH ₃ Flow rate	100%, 10 mL/min, 10% NH ₃ (V/V) in He
N ₂ O Flow rate	100%, 1.5 mL/min
Octopole RF	160 V
Octopole bias	- 8.5 V
Axial acceleration	2 V
Energy discrimination	- 18.0 V
Deflect lens	- 4.0 V

2.3 Radiochemical separation optimization

A radiochemical separation method was used to separate Cs from other elements that may cause interferences on ¹³⁵Cs and ¹³⁷Cs. The radiochemical method builds on previous published methods (Zheng et al, 2014, Zheng et al, 2016, Yang et al, 2016) and is divided into three main steps: extraction by sorption on ammonium molybdophosphate hydrate (AMP), anion exchange resin and cation exchange resin.

2.3.1 Step 1: AMP sorption + separation

The first step of radiochemical separation aimed to extract Cs using AMP. For the optimization of this step a simulated solution containing stable cesium and a variety of elements was used. The different sub-steps within step 1 are shown in Figure 2.1. The optimization of AMP mass used in step 1-1 and the technique used to separate the AMP from the solution were tested

and optimized. Studies conducted by C.J Miller for Idaho National Engineering Laboratory showed that AMP has a high selectivity and adsorption capacity towards Cs at low pH (i.e., pH < 2) (Miller, 1995), Under these conditions, AMP will form insoluble heteropolyacid salts with Cs and thus separating from other ions that do not attach to the AMP. Using AMP on inert carriers, like those used in anion- and cation exchange resins, will improve the sorption of Cs thanks to the advantages of carrying out a separation on a chromatography column (Miller, 1995). In basic solutions, AMP will dissolve (Miller, 1995), freeing Cs from the AMP compound. This allows to separate Cs from solutions with high contents of other elements such as Ba, which is an isobaric interference towards Cs. Therefore, the purpose of this step was: 1) test the amount of AMP needed for a satisfactory recovery of Cs and 2) check different solid solution separation methods to view their advantages and disadvantages. Three different concentrations of AMP (1, 5 and 10 mg/mL) were used, and paper filter, centrifugation and syringe filter units were tested as separation methods.

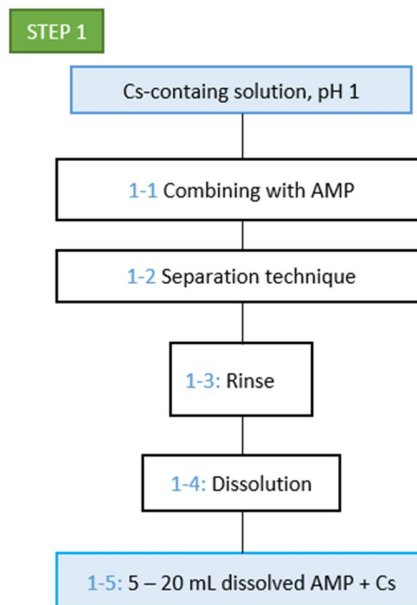


Figure 2. 1: Step 1 of the radiochemical separation comprising the sorption of Cs on AMP, separation from the solution and dissolution of the AMP.

In step 1-1, 20 mL of simulated solution (at pH 1) were mixed with AMP in 50 mL centrifuge tubes (VWR Ultra High Performance). These tubes were used because the AMP would not stick onto the walls of the tube. For blank samples, 20 mL of 1 M HNO₃ were used. The AMP was

weighted directly into the centrifuge tubes using a 4-decimal scale (Mettler Toledo AX204) before adding the simulated solution and mixing on a roller table for 30 to 60 minutes. The following AMP concentrations were tested in duplicate: 1, 5 and 10 mg/mL of added solution. Thus, 6 simulated solution samples (3 pairs of different AMP concentration) and 3 blank samples (each with a different concentration) were tested.

In step 1-2, centrifugation, filter paper and syringe filters were tested as methods for the separation of AMP from solution. The filter paper method included a Whatman paper filter (20-25 μm pore size, 100 mm diameter, cellulose filter) and a funnel, where the samples from step 1-1 were passed through by gravity. The AMP was retained on the filter, while the liquid was collected for analysis in case it still contained Cs. The filter with AMP was rinsed with 10 mL 1.0 M HNO_3 (step 1-3) followed by 5 to 15 mL (depending on AMP concentration) of 1.5 M NH_4OH to dissolve the AMP (step 1-4). While adding the NH_4OH , the AMP was mixed continuously with a spatula to increase dissolution. Dissolved AMP was collected into new centrifuge tubes (step 1-5).

For the centrifugation method, the AMP-containing samples were centrifuged (Beckman Coulter Allegra 64R centrifuge) for 10 minutes at 10,000 RCF. This time was sufficient to separate the yellow AMP (settled at the bottom of the centrifuge tubes) from the supernatant, which was transferred to another tube using a Pasteur pipette. The supernatant was kept for Cs analysis. As this method did not involve a filter, it was not possible to rinse the AMP before dissolving with NH_4OH (8 to 15 mL were used depending on the AMP concentration used and how much supernatant was removed).

For the syringe method, 0.45 μm filter units (polyethersulfone, VWR) and 20 mL plastic syringes (Henke Sass Wolf) were used. The samples were pushed through the filter by applying manual force. AMP was retained in the filter unit and the filtered liquid was collected for Cs analysis. The filter was rinsed with 10 mL HNO_3 (step 1-3), followed by 7 to 18 mL of NH_4OH to dissolve the retained AMP (step 1-4). The NH_4OH filtrate was added to the syringe and passed through the filter several times until full dissolution of the AMP (indicated visually by the progressive disappearance of the yellow color on filter).

2.3.2 Steps 2 and 3: Anion and cation exchange resins

Once the Cs has been extracted from solution with AMP, the NH_4OH solutions were subjected to another two steps using anion and cation exchange resins, as shown in Figure 2.2 (steps 2 and 3, respectively). These steps aimed to remove interfering anions and cations from the sample matrix that could interfere with measurement by ICP-MS. In step 2, the anion exchange resin was tested to mainly check for the decontamination factor of Mo. AMP has a high concentration of Mo, which is undesirable to transfer to the ICP-MS as it is hard to flush out. In step 3, the cation exchange resin was mainly checked to evaluate the decontamination factor of isobaric interfering elements such as Ba.

The anion (BioRad AG 1-X4 Resin, chloride form, Biotechnology grade, 100-200 mesh) and cation exchange (BioRad AG 50W-X8, hydrogen form, analytical grade, 100-200 mesh) resins were loaded into 2 mL resin bed gravity flow columns (Thermo Scientific) with frits placed above and beneath the resins. Funnels (30 mL) were placed on the top of the columns for better solution loading. To avoid cross contamination between samples, resins were not reused in this work, i.e., fresh columns were prepared for each sample.

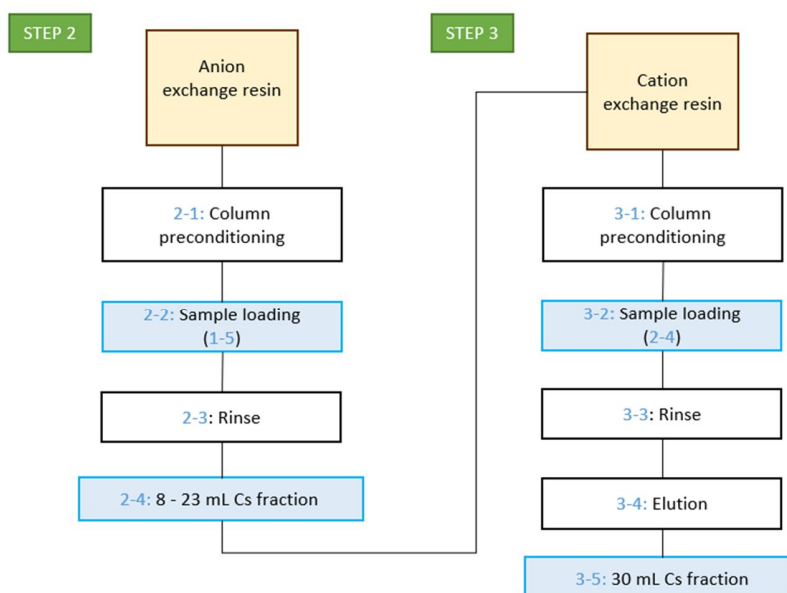


Figure 2. 2: Steps 2 and 3 of radiochemical separation including anion and cation exchange resin in columns to purify sample containing Cs.

In step 2-1, the anion exchange resin was first preconditioned with 10 mL MilliQ water, followed by 10 mL 1.5 M NH_4OH . In step 2-2, the dissolved AMP with Cs (in HNO_3 , pH 1) was passed through the column and the filtrate was collected, while most of the dissolved anions are retained in the resin. The column was rinsed with another 3 mL 1.5 M NH_4OH in case some Cs was still retained in the resin (step 2-3). The rinse was combined with filtrate from step 2-2, and a 200 μL aliquot was taken for later analysis by ICP-OES. The flow rate through the columns was often slow in the beginning and varied between columns, as they may not have been totally identical. Approximately 20 – 25 mL/h was generally measured.

In step 3, the cation exchange column containing AG 50W-X8 resin was first preconditioned (step 3-1) by passing through 10 mL 1.5 M HCl , followed by 10 mL MilliQ water and lastly 10 mL 1.5 M NH_4OH . After loading the sample (step 2-4) into the resin (step 3-2), the column was then rinsed with 10 mL 1.5 M HNO_3 followed by 10 mL MilliQ water (step 3-3). The rinse from step 3-3 was collected for later analysis in case Cs had not been retained in the column. Retained Cs was eluted with 30 mL 1.0 M HNO_3 (step 3-4) and collected into new centrifuge tubes. The flow rate through the resin was comparable to the anion exchange resin columns used in step 2. Both resins had the same mesh size (100 - 200) and the columns contained an equal amount of resin. The final volume of the sample was 30 mL in pH 1 and contained the eluted Cs from the cation exchange resin and was ready for ICP-MS analysis.

Additionally, another set of simulated solution samples went through the radiochemical protocol, but step 2 was skipped (i.e., solution from step 1-5 was loaded directly into the cation exchange resin (step 3-2)). This test allowed to evaluate any major effect on the separation of anions from the samples, most importantly Mo.

2.3.3 Decontamination factor and recovery

Aliquots of 0.2 mL of the simulated solution and blank samples taken at the different steps of the radiochemical separation (i.e., step 2-4) were diluted to 10 mL with 1.0 M HNO_3 and measured by ICP-OES for Al, Ba, Ca, K, Mg, Mo, and Na concentration. This allowed to estimate the decontamination factor (DF; equation 3; (Kumar et al., 2010)) for these elements by the first radiochemical separation steps 1 and 2.

$$DF = \frac{\text{Contamination level of material or component before the decontamination application}}{\text{Contamination level measured immediately after decontamination application}}$$

(Equation 3)

The recovery of the radiochemical separation (equation 4) for stable Cs and the decontamination factor for Ba was estimated from Cs and Ba concentrations determined in the diluted aliquots by QQQ-ICP-MS.

$$\% \text{ Recovery} = \frac{\text{Concentration of Cs collected after separation}}{\text{Initial concentration}} * 100\%$$

(Equation 4)

2.4 Optimization of soil digestion

After the optimization of the radiochemical separation steps the microwave-assisted acid digestion of soil samples was tested. This allowed to check if there was any difference in digestion and recovery of Cs from the soil samples. Two different acid mixes were used. Acid mix 1 was supposed to be easier to use, while acid mix 2 was supposed to digest better, but produces more hazardous waste.

2.4.1 Acid mix digestion test

The digestion efficiency of two different acid solutions were tested with dried soils from 5 different locations within the Fukushima exclusion zone (Table 2.3) that contained an organic content ranging from 15 to 50%. Duplicated soil samples (ca. 0.5 g) were accurately weighted into LSC polyethylene vials on a 4-decimal scale and measured for ¹³⁷Cs in the NaI-detector. After NaI-detector analysis, the soil samples were transferred into acid-washed Teflon tubes, and the weight was again accurately recorded (in case of mass loss during transfer). Subsequently, the following acid concentrate solutions were added to the soils (one to each duplicate samples):

- Acid mix 1: 5 mL HNO₃
- Acid mix 2: 2.5 mL HNO₃ + 5 mL H₃PO₄ + 2.5 mL HBF₄

Soil samples were then digested in the UltraWave. After cooling down, the digested samples were transferred into 15 mL centrifuge tubes by decanting the contents and rinsing the Teflon tubes 3 times with MilliQ water. The centrifuge tubes were filled to the 15 mL mark with MilliQ water and left to settle until the next day. Pictures of sediment was taken the day after. After sedimentation, 5 mL of the digested solutions were transferred to LSC vials using a Pasteur/Micropipette and measured for ^{137}Cs in the NaI-detector. This allowed to calculate the recovery of ^{137}Cs of the digestion of the different acid mixes.

2.4.2 Re-testing step 2 – anion exchange resin

Step 2 of the radiochemical separation (i.e., anion exchange resin) was tested again with digested soil samples to evaluate any matrix effect on the separation, i.e., to check if the anion exchange resin was necessary for obtaining samples with satisfactorily low concentrations of interfering anions.

To do this, 6 replicates of soil 18b (ca. 0.5 g,) and 6 blank samples were weighted into LCS vials and measured in the NaI-detector for ^{137}Cs . Samples were then digested with acid mix 1 (5 mL HNO_3) in Teflon-tubes in the UltraWave. After digestion, the Teflon tubes contents were decanted into 15 mL centrifuge tubes and diluted to 15 mL with MilliQ water. After sedimentation (> 48 h), 13 mL of the supernatant were transferred to LSC vials for measurement on the NaI-detector to calculate the ^{137}Cs recovery. Subsequently, 3 digested soil replicates and 3 blank replicates were subjected to the radiochemical separation from step 1 through 3 as described in section 3.3, whereas the other 3 soil and 3 blank replicates went through the radiochemical separation without step 2. In both cases, 1 mg/mL of AMP and a syringe with a 0.45 μm filter unit were used in step 1). After the radiochemical separations, i.e., with and without step 2, the samples were analyzed by ICP-MS to determine the concentration of ^{137}Cs and ^{133}Cs and other elements such as Al, Ba, Fe, Mo, Mg, Mo, P and Rb.

2.5 Fukushima samples

2.5.1 Sample details and preparation

Table 2.3 lists the bulk soil and sequential extraction samples used in this study. A complete table for samples collected in Fukushima exclusion zone can be found in (Reinoso-Maset et al.,

2020). There were various sampling sites ranging from 1291 m to 10561 m from the nuclear power plant in south, west, and north directions. The samples are labeled with sampling site numbers that indicate which site the sample was taken from, and the sample site letters indicate the different samples from the same area. The samples were mostly taken from soil with a depth of 0 to 20 cm. There were also samples composed of gravel, sand, and sediment. The range of organic content varied, ranging from 2.9% to 50%. Samples used in this study were thoroughly homogenized, freeze dried and sieved to < 2 mm fraction prior to use (Reinoso-Maset et al., 2020).

Additionally, leachates from step 6 of sequential chemical extraction carried out by (Tetteh, 2018) were also analyzed. These samples were obtained in the last step of the chemical extraction by leaching 2 g of soil with 20 mL of 7 M HNO₃ at 80 °C for 6 h. The ¹³⁷Cs activity concentration in these samples have been previously determined by gamma spectrometry using a NaI-detector (Tetteh, 2018).

For the determination of ¹³⁵Cs and ¹³⁷Cs, the bulk soil and the sequential extraction samples were prepared in triplicate. Dried soils were accurately weighted (ca. 0.5 g) into LSC vials with a 4 decimal balance and measured in a NaI-detector to determine the initial ¹³⁷Cs activity concentration. The soils were then transferred to Teflon tubes, accurately weighed, and 5 mL concentrated HNO₃ were added for microwave digestion in the UltraWave. All digestion contents from were transferred to centrifuge tubes, Teflon tubes were rinsed with MilliQ water, and digested samples were then diluted to 15 mL with MilliQ water and let to settle for 24 hours to separate undigested solids. The solutions were pipetted out into LSC-vials and measured again for ¹³⁷Cs in the NaI-detector to calculate the recovery of ¹³⁷Cs from the digestion. The optimized radiochemical separation was then applied to these digested soil samples followed by QQQ-ICP-MS analysis. Additionally, four blank samples composed of only concentrated HNO₃ were also prepared and underwent the same digestion, radiochemical separation, and analyses as the samples. The measured concentrations were used to calculate LOD and LOQ for ¹³⁵Cs and ¹³⁷Cs. The sequential extraction samples (20 to 34 mL) went directly through the optimized radiochemical separation, as these samples were in a liquid state at the optimal pH and matrix for radiochemical separation and required no previous treatment.

Table 2. 3: Sample details for Fukushima soil samples. Samples were collected by NMBU staff on field trip to Fukushima in September 2016 (Reinoso-Maset et al., 2020). Details include distance to reactor from sampling site, wind direction, general depiction of sample site, type of sample, depth of collection and the organic content. The sequential extraction samples (step 6, 7 M HNO₃) were obtained by Tetteh, 2018. Original label names are shown together with the correspondence to the bulk sample numbers in brackets.

Label	Distance, m	Windrose	Location	Type	Depth, cm	Organic content, %
<i>Bulk soil samples</i>						
1b	1452	WNW	Northwest of reactor, transect between Inkyozaka pond and FDNPP	soil	0 - 3	21
3	1375	WNW		soil	0 - 3	33
6a	2371	SSE	South of reactor, forest by the sea	soil	0 - 6	47
7a	1541	SSE	South of reactor, concrete platform next to fish factory by the sea	soil/gravel/sand	0 - 5	5
8	1452	WNW	Northwest of reactor, ditch (concrete) outside a house	fine/grained soil	surface	15
9b	7842	WSW	West of reactor, road into forest, near graveyard	soil/gravel	0 - 5	2.9
10c	7832	WSW		soil in grass field	0 - 6	7.8
14	1291	SSW	Southwest of reactor, Okuma town	sandy soil	mid layer	n/a
16b	1464	WNW	Northwest of reactor, Inkyozaka pond between forest and FDNPP	sediment	surface	8.6
16c	1464	WNW		soil	n/a	34
16n	1464	WNW		soil	0 - 5	8.1
17-3	10561	WNW	Northwest of reactor, by Omaru shrine	soil	0 - 20	50
17-v	10561	WNW		soil	0 - 20	n/a
18b	4690	WSW	Suzuuchi pond	soil	surface	14
<i>Sequential extraction samples [step 6, (fraction 6)]</i>						
SR1 (7a)	1541	SSE	South of reactor, concrete platform next to fish factory by the sea	soil/gravel/sand	0 - 5	5
HP1 (8)	1452	WNW	Northwest of reactor, ditch (concrete) outside a house	fine/grained soil	0 - 6	15
TR1B (10c)	7834	WSW	West of reactor, road into forest, near graveyard	soil in grass field	0 - 5	7.8
HT2 (13)	1349	SSW	Southwest of reactor, outside a house	soil	n/a	11
INP (16b)	1464	WNW	Northwest of reactor, Inkyozaka pond between forest and FDNPP	surface	sediment	8.6
INS6 (16n)	1464	WNW	soil	soil	0 - 5	8.1
SUZ (18)	4690	WSW	West of reactor, Suzuuchi fishpond	soil	surface	14

2.5.2 $^{135}\text{Cs}/^{137}\text{Cs}$ isotope ratio measurements

To evaluate if there were high concentrations of elements that could interfere with the measurements on the QQQ-ICP-MS with an ApexQ-nebulizer, the digested soil sample 18b was measured after radiochemical separation on an Agilent 8800 ICP-MS and various elements were screened. The ApexQ nebulizer has a much higher efficiency than regular nebulizers and requires significantly less volume of injected sample (*Apex Q Desolvating Nebulizer*, 2021). After the screening, the rest of the Fukushima soil samples (Table 2.3) were measured in the Agilent 8900 ICP-MS for Ba, ^{133}Cs , ^{135}Cs and ^{137}Cs . The method included 7 replicate measurements per sample. Indium ($1\ \mu\text{g}/\text{L}$; prepared from $10\ \text{mg}/\text{L}$ standard solution, Inorganic Ventures) was used as internal standard by adding an aliquot to the samples after radiochemical separation. A $200\ \mu\text{g}/\text{L}$ Ba standard solution ($10\ \text{mg}/\text{L}$, Inorganic ventures) was used as an interference check and to calculate the background equivalent concentration (BEC).

The mass bias factor for the isotopic ratio of ^{135}Cs and ^{137}Cs was determined using another element. Several elements, such as Ag, Sb and Rb were evaluated, but Sn was found to be the more suitable element. Tin isotopes ^{122}Sn and ^{124}Sn have a similar mass to ^{135}Cs and ^{137}Cs and are inert towards the reaction gases used during the ICP-MS measurement (i.e., N_2O and NH_3). When measuring $25\ \mu\text{g}/\text{L}$ Sn with In as internal standard, a mass bias correction of 1.012 was obtained. The same mass bias correction was then applied to obtain the $^{135}\text{Cs}/^{137}\text{Cs}$ isotope ratio.

During the measurement of the soil samples after applying the optimized radiochemical separation, the internal standard signal decreased severely and thus the ICP-MS was stopped in the middle of the run. The ApexQ-nebulizer was unplugged from the instrument and checked. The tubes and filter were clogged with a white powder and a brown slurry-type precipitate. The white powder was most likely residues of the resin. In order to continue with the measurements, a regular pneumatic concentric nebulizer was connected, and the ICP-MS re-tuned for the method. This nebulizer did not compromise the analysis in regards of the internal standard signal and thus was used for the remainder of the samples. The change in performance was worse as the sensitivity was low compared to the Apex-Q nebulizer. All data in results section were obtained with the pneumatic concentric nebulizer.

3. Results and discussion

3.1 Method optimization

3.1.1 Evaluating the matrix

Since the soil samples from Fukushima were expected to have high concentrations of other ions than Cs, a simulated solution was prepared to test the radiochemical separation method for removing ions that could interfere with the detection of Cs. Three different separation methods were used in step 1 of the radiochemical separation, namely paper filter, centrifuge, and syringe with filter. Within these separation methods, three different concentrations of AMP ranging from 1 to 10 mg/mL were used. The objective of this test was therefore to check if the decontamination factor (DF) varied between the separation methods and the use of AMP, as well as to check if step 2, the anion exchange resin, had a major impact on removing ions. Table 3.1 shows the concentration of elements of interest and the associated decontamination factor for the different steps used in the radiochemical separation measured by ICP-OES. Samples labelled as “aliquot” were those collected after step 2 of the radiochemical separation, whilst the other samples were collected after the full procedure.

The LOD of the elements were ranging from 0.0012 to 0.527 mg/L, and the LOQ was ranging from 0.004 to 2.05 mg/L. The LOQ for K was however at a higher concentration (2.03 mg/L) than the initial calculated concentration of 1.02 mg/L, thus it would not be considered as an acceptable level. In the same manner, the LOQ for Mo was also high, at a concentration of 2.05 mg/; but due to the initial high concentration of Mo in the samples, a LOQ of that magnitude is usable and considered low. The high LOQ of K and Mo might be due to low instrumental sensitivity of the ICP-OES towards those elements, or it could be that the blank samples contained some “dirt” from the radiochemical separation method. For the rest of the elements, especially Ba, the LOD and LOQ (0.0012 mg/L and 0.004 mg/L respectively) is considered low and suitable for the analyses in this study.

Table 3. 1: Concentrations and decontamination factors (DF) for Al, Ba, Ca, K, Mg, Mo and Na measured by ICP-OES in simulated solution samples after the full radiochemical separation procedure and after step 2. Sample names indicate step 1 separation method (i.e., paper filter, centrifuge, syringe) and amount of AMP (i.e., 1, 5 or 10 mg/mL). Reported DF values are based on measured concentrations or the ratio of the method's detection and quantification limits (LOD/LOQ; based on method blanks) for each element.

<i>Element</i>	<i>Al</i>		<i>Ba</i>		<i>Ca</i>		<i>K</i>		<i>Mg</i>		<i>Mo</i>		<i>Na</i>	
Sample	mg/L	DF	mg/L	DF	mg/L	DF	mg/L	DF	mg/L	DF	mg/L	DF	mg/L	DF
<i>Initial concentration</i>	100		5.27		16.2		1.02		4.02		*		10.4	
<i>LOD</i>	0.052		0.0012		0.527		0.609		0.182		0.615		0.242	
<i>LOQ</i>	0.174		0.0040		1.76		2.03		0.61		2.05		0.808	
After full separation														
Paper filter 1 AMP	<LOQ	574	<LOD	4446	<LOQ	9	<LOD	1.7	<LOD	22	<LOD	991	<LOQ	13
Paper filter 5 AMP	<LOQ	574	<LOQ	1334	<LOQ	9	<LOD	1.7	<LOD	22	<LOD	4957	0.84	12
Paper filter 10 AMP	<LOQ	574	<LOQ	1334	<LOQ	9	<LOD	1.7	<LOQ	7	<LOD	9913	0.84	12
Centrifuge 1 AMP	<LOQ	574	0.005 ± 0.002	1253 ± 115	<LOQ	9	<LOD	1.7	<LOQ	7	<LOD	991	0.8 ± 0.4	12.5 ± 0.4
Centrifuge 5 AMP	<LOQ	574	<LOQ	1334	<LOQ	9	<LOD	1.7	<LOQ	7	4.35 ± 5.28 **	2667 ± 3238	<LOQ	13
Centrifuge 10 AMP	<LOQ	574	<LOQ	1334	<LOQ	9	<LOQ	0.5	<LOD	22	<LOD	9913	<LOQ	13
Syringe 1 AMP	<LOD	1912	<LOD	4446	<LOQ	9	<LOD	1.7	<LOD	22	<LOD	991	<LOD	43
Syringe 5 AMP	<LOD	1912	<LOD	4446	<LOQ	9	<LOD	1.7	<LOD	22	<LOD	4957	<LOD	43
Syringe 10 AMP	<LOQ	574	<LOQ	4446	<LOQ	9	<LOD	1.7	<LOD	22	<LOQ	2974	<LOD	43
After step 2														
Paper filter 1 AMP	0.5 ± 0.60	1011 ± 1274	0.04 ± 0.02	147 ± 68	<LOD	31	<LOD	1.7	<LOD	22	<LOD	991	<LOD	43
Paper filter 5 AMP	2.0 ± 1.6	96 ± 86	0.01 ± 0.01	515 ± 364	<LOQ	9	<LOD	1.7	<LOQ	7	460 ± 658	648 ± 911	<LOQ	13
Paper filter 10 AMP	2.7 ± 0.3	37 ± 4	0.043 ± 0.006	125 ± 18	<LOQ	9	<LOD	1.7	<LOQ	7	2200 ± 1460	4 ± 2	3.0 ± 2.7	5 ± 4
Centrifuge 1 AMP	0.3 ± 0.3	1052 ± 1216	0.057 ± 0.006	93 ± 6	<LOQ	9	<LOD	1.7	<LOD	22	LOD	991	<LOD	43
Centrifuge 5 AMP	0.5 ± 0.2	221 ± 115	<LOQ	1334	<LOQ	9	<LOQ	0.5	<LOQ	7	390 ± 555	2480 ± 3502	<LOQ	13
Centrifuge 10 AMP	0.6 ± 0.8	999 ± 1291	<LOD	4446	<LOD	31	<LOD	1.7	<LOD	22	2110 ± 142	2.9 ± 0.2	2.48 ± 0.03	4.18 ± 0.05
Syringe 1 AMP	0.1750 ± 0.0004	573 ± 1	<LOD	4446	<LOQ	31	<LOD	1.7	<LOD	22	<LOD	991	<LOD	43
Syringe 5 AMP	0.9 ± 0.2	106 ± 21	0.009 ± 0.001	617 ± 63	<LOQ	9	<LOD	1.7	<LOD	22	<LOD	4957	<LOD	43
Syringe 10 AMP	1.0 ± 0.1	99 ± 21	<LOD	4446	<LOD	31	<LOD	1.7	<LOD	22	<LOQ	2974	<LOD	43
With no step 2														
Syringe 1 - 10 AMP ***	<LOQ	574	<LOD	4446	<LOQ	9	<LOD	1.7	<LOD	22	LOQ	2974	<LOD	43

* Mo had a different initial concentration since AMP contains Mo: 610, 3050, 6100 mg/L for the 1, 5 and 10 AMP respectively

** Outlier, too high value not consistent with replicate samples

*** Average value for samples with 1, 5 and 10 AMP that had not gone through step2 of the radiochemical separation

In general, the concentrations of most elements for the three separation methods and after the full radiochemical separation were below the respective LOQ. Contrastingly, subsamples after step 2 of the radiochemical separation presented measurable concentrations over the LOQ for most elements. This suggests that the full radiochemical separation worked excellent in terms of removing major ions from the solution. In the case of K, it is hard to determine whether the radiochemical separation worked as there was a low initial concentration and a high LOQ. For Ba, a very important isobaric interference towards Cs, the analysis showed the lowest LOD and LOQ with 0.0012 and 0.0040 mg/L, yet the concentrations after the full separation and/or step 2 were detectable/below LOQ. Overall, the elements that showed the highest DF were Ba, Mo and Al. That is understandable, as Mo and Al had the highest initial concentrations with a relative low LOQ. As for Ba, the initial concentration was low, but had a very low LOD. Potassium was the element to show the lowest DF, as it could not be measured more accurately due to low initial concentration and high LOQ.

The AMP concentration used in step 1 had an effect on the DF of Mo. Increasing levels of AMP caused the DF of Mo to decrease (i.e., worse removal of ions) when using paper filter and centrifuge separation methods in step 1. As for the complete radiochemical separation, increasing levels of AMP caused the DF of Mo to be substantially better. For the syringe method, it seemed that the DF of Mo was the same after step 2 than after step 3, meaning that step 1+2 was able to remove the majority of Mo from solution. For the other elements, the concentration of AMP did not seem to affect the DF after the full radiochemical separation. Although subsamples in step 2 showed that increasing levels of AMP worsened the DF of Al for all separation methods, the levels of ion removal was still acceptable.

The DF after step 2 varied among elements. For Ba, much less was removed with the centrifuge and paper filter methods compared to the syringe method. For the rest of the elements, the DF was the same for step 1+2 as for the complete radiochemical separation, meaning that most of the concentration was removed in step 1+2 of the procedure.

Overall, the separation method used in step 1 that was most successful in removing ions from solution was the syringe method. This method resulted in the best in DF for most of the

elements after step 1+2 and after step 1+2+3, including a good/excellent DF for Ba, which is the most important element to remove. Moreover, it was much easier to work with compared to the paper filter and centrifuge method. The syringe and filter allowed for working in a closed environment and the ability to clean the syringe filter several times to dissolve as much AMP as possible, which contained the Cs. This proved much harder for the other separation methods. As for the centrifuge method, it was very hard to remove the supernatant without also removing the AMP. The paper filter could easily separate the AMP from the solution but was very hard to dissolve due to not being able to use “infinite” amounts of liquid as you could for the syringe filter method.

Therefore, based on these results and observations, the syringe method will be applied to the soil samples. As for step 1+2, it would be interesting to know if it is the physical separation in step 1 or the anion resin exchange in step 2 that has the biggest impact on the removing of major ions. To save time, step 2 could be dismissed, but only if the decontamination of the samples is considered good enough, meaning that the concentrations left in the solution would not interfere with the measurement of Cs by ICP-MS.

3.1.2 Removing interfering ions

The DF of elements of interest were determined by ICP-OES at different steps of the radiochemical separation in order to check the capability of the method to remove interfering ions. The recovery of Cs after the radiochemical separation is also an important factor to evaluate the method as is to know if higher levels of AMP increase the recovery percentage. To evaluate the recovery at the different steps of the radiochemical separation, the same samples from table 3.1, i.e., samples after steps 1+2 and after steps 1+2+3, were measured by ICP-MS. Here, Ba was checked again to determine the DF. It is worth to mention that concentrations calculated for step 2 were obtained from 0.2 mL aliquots diluted to 10 mL, whilst the concentrations after the full radiochemical separation were measured directly in the final 30 mL sample.

Figure 3.1 shows the Cs and Ba concentrations (in $\mu\text{g/L}$) measured in samples that underwent the 3 steps of the radiochemical separation or just the first 2 steps (Figure 3.1A and 3.1B

respectively), with different separation method in step 1, i.e., paper filter, centrifugation and syringe filter, and different levels of AMP ranging from 1 to 10 mg/mL of sample volume. In general, for all separation methods, the concentration of Cs was ranging from 7.1 to 11.3 $\mu\text{g/L}$ after the full 3 steps, whilst the concentration Ba was ranging from 1.0 to 3.7 $\mu\text{g/L}$. For step 2, the concentrations of Cs and Ba were ranging from 6.8 to 11.3 $\mu\text{g/L}$ and from 2.0 to 50 $\mu\text{g/L}$, respectively. The instrumental LOD and LOQ for Cs was measured to be 0.0009 $\mu\text{g/L}$ and 0.0031 $\mu\text{g/L}$ respectively, obtained by using data from wash samples. 9 method blank samples were used to determine the method LOD and LOQ, which showed 0.424 $\mu\text{g/L}$ and 1.412 $\mu\text{g/L}$ respectively. For Ba, the instrumental LOD and LOQ was 0.0401 $\mu\text{g/L}$ and 0.1336 $\mu\text{g/L}$ and the method LOD and LOQ was 0.154 $\mu\text{g/L}$ and 0.514 $\mu\text{g/L}$ respectively.

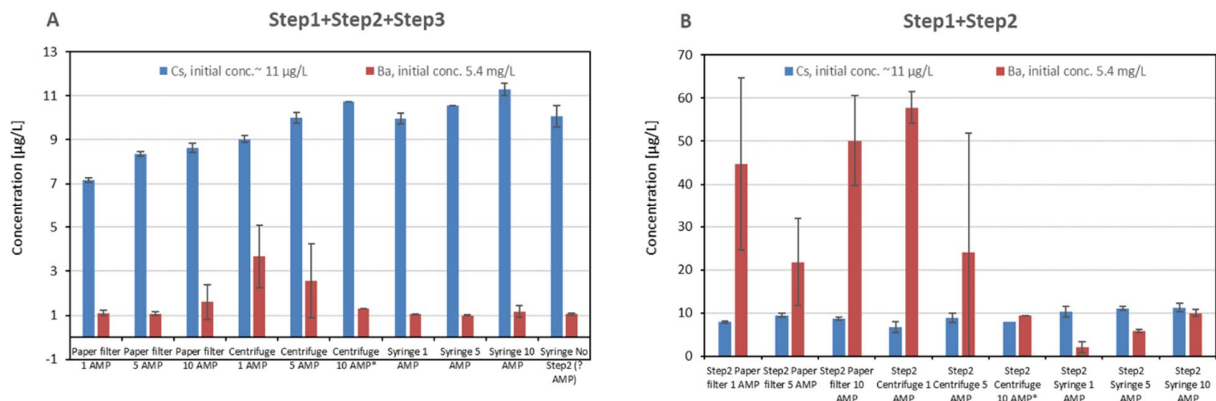


Figure 3. 1: Concentrations of Cs and Ba (in $\mu\text{g/L}$) in the simulated solution after steps 1, 2 and 3 of the radiochemical separation (A) and after steps 1 and 2 only (B), using 3 different types of separation in step 1 (paper filter, centrifugation, and syringe + filter) and 3 different concentrations of AMP (1, 5 and 10 mg/mL). Error bars represent the standard deviation of duplicate samples (* = one replicate). Note the different scale for Ba concentrations in A for samples after steps 1 and 2.

Figure 3.2 shows the recovery of Cs respect to the initial added concentration for all separation method (paper filter, centrifuge, and syringe filter) with a range of 1 to 10 mg AMP /mL after the full radiochemical separation (steps 1+2+3) and after the first 2 steps (steps 1+2). The range of recovery for Cs was in between 66 and 101% in general for the 3 separation methods after the full 3 steps. After 2 steps, the recovery of Cs was between 61 and 101%.

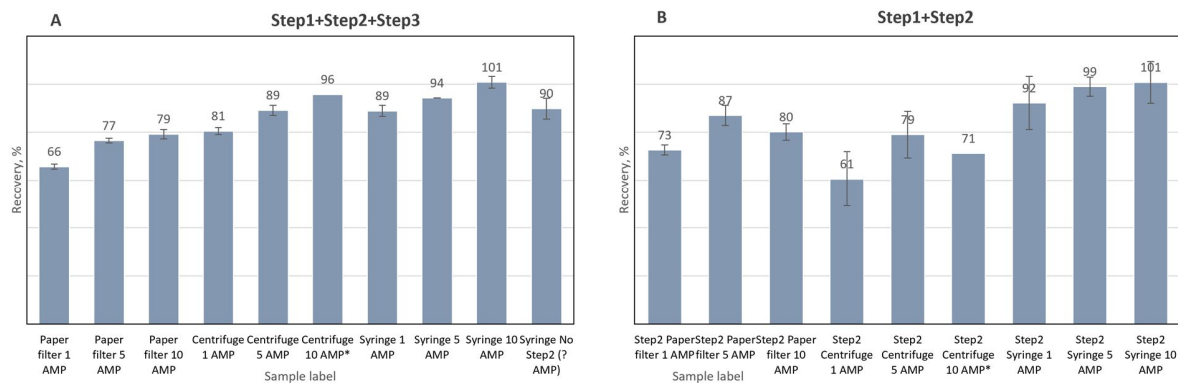


Figure 3. 2: Recovery of ¹³³Cs (in %) in simulated solution after 3 steps of the radiochemical separation (A) and after step 1 and step 2 only (B), using 3 different types of separation in step 1 (paper filter, centrifugation, and syringe + filter) and 3 different concentrations of AMP ranging from 1 to 10 mg/mL. Error bars represent the standard deviation of duplicate samples (* = one replicate).

Figure 3.3 shows the DF of Ba for the 3 separation methods used and after the 3 steps of radiochemical separation or after only 2 steps (Figure 3.3A and 3.3B respectively). The range of DF of Ba was between 1603 to 5347 for the full 3 steps, where most of the values were between 4000 and 5000. After step 2 most DF values were in the low hundreds, except for step 2 syringe 1 AMP, which had a significantly higher DF than the other samples. The total range for DF of Ba was between 94 and 3132.

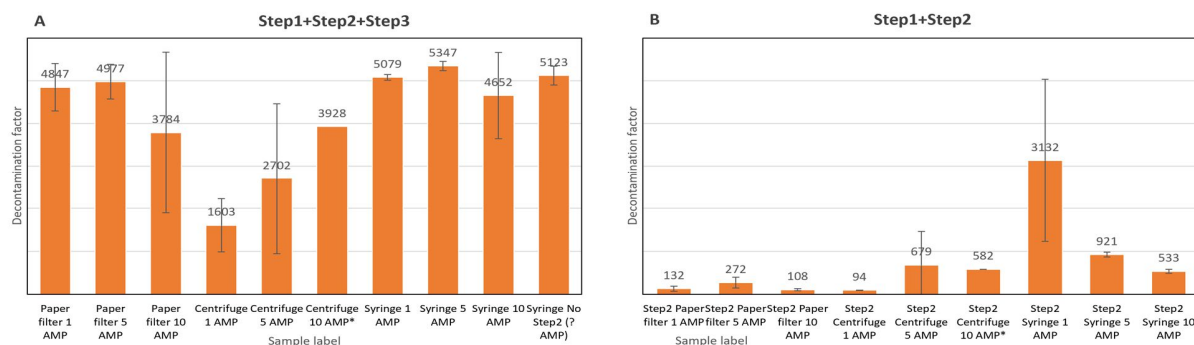


Figure 3. 3: Decontamination factor of Ba in simulated solution after 3 steps (A) and after step 1 and 2 only (B) of the radiochemical separation, using 3 different types of separation in step 1 (paper filter, centrifugation, and syringe + filter) and 3 different concentrations of AMP ranging from 1 to 10 mg/m L. Error bars represent the standard deviation of duplicate samples (* = one sample).

The syringe filter separation methods resulted in the highest concentration of Cs ranging from 10.0 to 11.3 µg/L with an average of 10.6 ± 0.6 µg/L, meaning a recovery between 90 to 101% (average of 95 ± 5.5 %) after the full radiochemical separation. The difference between the 6

replicates was acceptable, with an RSD of 5.9% for the Cs concentration. After step 2, the range of concentration was between 10.3 and 11.3 $\mu\text{g/L}$ and an average of $10.9 \pm 0.9 \mu\text{g/L}$. The calculated recovery ranged from 92 to 101% with an average of $97 \pm 7.7\%$ of the initial concentration of 11.2 $\mu\text{g Cs/L}$. In this case, the uncertainty was slightly higher, with 7.9% between the 6 replicates. The syringe filter separation method also resulted in a low concentration of Ba. At the end of step 3, the Ba concentration was ranging from 1.0 to 1.1 $\mu\text{g/L}$. This resulted in a DF of Ba after step 3 ranging between 4662 to 5347, with an average of 5026 ± 553 , and a 13% RSD between the replicates. After step 2, the concentration of Ba was between 2.1 and 10 $\mu\text{g/L}$, giving a DF range between 44 to 1904, with an average of 1529 ± 1516 and an RSD of 61%.

Among the samples using the syringe filter method of the radiochemical separation, there were 3 replicates that did not undergo step 2 of the procedure but only steps 1 and 3. In these samples, the Cs concentration ranged from 9.5 to 10.6 $\mu\text{g/L}$, with an average of $10.0 \pm 0.5 \mu\text{g/L}$ (4.8% RSD) and $90 \pm 4\%$ recovery. The concentration of Ba was ranging from 1.0 to 1.1 $\mu\text{g/L}$ with an average of $1.04 \pm 0.05 \mu\text{g/L}$ (4.5% RSD), which gives an average DF of 5123 ± 220 .

The centrifugation method resulted in similar but lower concentrations of Cs compared to the syringe method, ranging from 9.0 to 10.7 $\mu\text{g/L}$ with an average of $9.7 \pm 0.7 \mu\text{g/L}$ after step 3. This results in an average recovery of $87 \pm 7\%$ (range from 81 to 96%). One replicate of the “centrifuge 10 AMP” sample had no measurable Cs, yet the Cs concentration of the remaining 5 replicates were within a 7.6% uncertainty, which is comparable to the syringe filter method. The concentration of Cs after step 2 presented a lower recovery than for step 3, with concentrations in the range of 6.8 to 8.9 $\mu\text{g/L}$ (17% RSD), yielding a range of 61 to 79% (average of $70 \pm 12\%$). Although the Cs recovery was good after step 3, the concentration of Ba was substantially higher for this method (1.3 - 3.7 $\mu\text{g Ba/L}$, average of $2.7 \pm 1.4 \mu\text{g Ba/L}$, 52% RSD) compared to the syringe filter method. Although it might initially seem like a poor result, the DF of Ba after step 3 ranged from 1603 to 3928 (increasing with AMP levels), with an average of 2508 ± 1342 . As for after step 2, the concentration of Ba was between 9.3 to 58 $\mu\text{g/L}$, giving a DF range between 94 to 679, where 5 and 10 mg/mL AMP samples had 6-7 times higher value

than the sample with 1 mg/mL AMP. The average DF of Ba after step 2 was 426 ± 407 (RSD of 75%).

The paper filter method presented the lowest concentration of Cs, ranging from 7.1 to 8.6 $\mu\text{g/L}$ after step 3 with an average of $8.0 \pm 0.7 \mu\text{g/L}$. That results in a recovery range of 66 to 79% with an average of $74 \pm 6\%$. The RSD for Cs concentration was 8.8%. The Cs concentration after step 2 was substantially higher compared to step 3, with an average of $8.7 \pm 0.7 \mu\text{g/L}$ (8.7% RSD) and a range between 7.9 to 9.6 $\mu\text{g/L}$. This resulted in a recovery range of Cs between 73 to 87% with an average of $80 \pm 7\%$. The measured concentration of Ba was between 1.1 to 1.6 $\mu\text{g/L}$ after step 3, giving an average of $1.2 \pm 0.4 \mu\text{g/L}$ (36% RSD). For this step, the DF of Ba was good, with an average of 4536 ± 1073 and a range between 3784 and 4977. After only step 2, the concentration levels of Ba were higher than for after step 3, with a range between 21.8 and 50.1 $\mu\text{g/L}$, giving an average of $39 \pm 17.4 \mu\text{g/L}$ and RSD of 45%. These high concentrations resulted in lower DF levels, with a range from 108 to 272 and an average of 170 ± 101 .

In general, the syringe filter method gave the highest DF for Ba for all concentrations of AMP. When comparing the DF of Ba for each separation method but same AMP concentration, paper filter and syringe filter had almost the exact same value when using 1 mg/mL AMP at ca. 5000, while the DF value dropped to 1600 for the centrifuge samples. Although this value is lower compared to the other methods, it is still acceptable. The same trend can be seen in the 5 mg/mL AMP samples, where paper filter and syringe filter methods resulted in values in the 5000 range, whilst only a 2700 DF were achieved with the centrifuge method (note the very large uncertainty in the measurements). For 10 mg/mL AMP, results show almost the same DF of Ba for both paper filter and centrifuge methods. In this case, the uncertainty of the result for the paper filter samples was large and overlaps with the range of DF values at ca. 5000 obtained with 1 and 5 mg/mL AMP. These samples were only carried out in duplicate, and that might be the reason for such a big standard deviation in the measurements. The results for the syringe filter method using 10 mg/mL AMP were comparable with the 1 and 5 mg/mL AMP samples, again with the DF in the 5000 range. It is interesting to note that the samples with no step 2 and AMP concentrations from 1-10 mg/mL also had ca. 5000 DF for Ba, suggesting that the AMP might not have an impact on the DF of Ba in the radiochemical separation method. As

for the other methods, the paper filter also does not show any major differences in Ba DF between the different AMP levels. However, the AMP concentration had an effect when the centrifuge method was used. In this method, the supernatant was pipetted out from the centrifuge tube after the step 1, which could potentially lead to not removing all the supernatant before dissolving the AMP with NH_4OH . Both paper filter and syringe methods used a type of filter to drain the solution out, which likely contains most of the initial Ba. The results also showed large differences between replicates of the centrifuge method, resulting in high uncertainties for both recovery of Cs and DF of Ba. Therefore, it is difficult to conclude whether the AMP levels did not impact the DF of Ba when using the centrifuge method.

The results show a general trend that increasing levels of AMP slightly increased the recovery of Cs from 10 to 15% for all separation methods and 1, 5 and 10 mg/mL AMP. When comparing the recovery of the different separation methods, the syringe method was undoubtedly the best independently of the AMP concentration, ranging from 89 to 101%. The centrifuge method resulted in slightly lower recovery than the syringe filter method by only a few percent points, ranging from 81 to 96%. The paper filter presented the lowest recovery in general, with a range between 66 to 79%. This might be explained by the step 1 process, where the filter was rinsed with NH_4OH to dissolve the AMP and, since the filter was rather fragile, a fraction of the AMP flowed and stuck to the sides and bottom of the filter, making it hard to dissolve everything on the filter. In contrast, when using the syringe connected to a filter unit, which was much smaller than the paper filter and was contained within the plastic case, the same amount of NH_4OH could be pushed through repeatedly until the filter was visibly clean (AMP is bright yellow). This repeated rinsing was not possible with the paper filter method, as it would use too much NH_4OH . Therefore, it can be expected that the recovery of the paper filter was lower than the syringe filter method.

Regarding differences in the Cs recovery between steps 1+2 and steps 1+2+3 samples, the results show a general trend of being slightly lower after step 2 than after step 3, especially for the centrifuge method (61-79% vs. 89-96%). This difference is unexpected because this would mean that Cs was added between step 2 and 3. The samples after step 2 were prepared by taking 0.2 mL aliquots and diluting to 10 mL, with all separation methods and different AMP

levels requiring a different amount of NH_4OH to dissolve the AMP. It can thus be assumed that the concentrations are underestimated because of uncertainties associated to the dilution step, resulting in samples with relatively low concentrations that are harder to detect and thus the data has higher uncertainty. Contrastingly, for the step 3 samples, the starting and ending solution volumes were the same, meaning less dilution and thus higher concentrations in solution with smaller associated measurement uncertainty.

On the other hand, there was a noticeable difference in DF of Ba between steps 1+2 and 1+2+3 samples. Besides the “step 2 syringe 1 AMP” samples that had over 3000 DF with a large uncertainty, most of the DF were between 100 and 1000 independently of the separation method applied. The syringe method also proved better here, whilst the paper filter method was worst. After step 3, the DF was 5 to 50 times higher than after step 2 (for all separation methods), and most notably for the paper filter method. Steps 1+2 resulted in good Ba DF values, ranging between 100 to 1000, but the significant decontamination of Ba occurred in step 3, where most DF levels were over 5000.

Considering the recovery and DF results for simulated solution samples with the different step 1 variations, the syringe method was certainly the best for radiochemical separation with a simulated solution. It resulted in the best recovery of Cs, the best DF of Ba, and it was the easiest to use. As for the levels of AMP, they did not affect the Cs separation by more than a 10% increase in recovery, meaning that 1 mg/mL AMP was enough to recover most of the Cs. Therefore, since AMP contains large amounts of Mo (61% of the molecule weight) and the soils samples to be analyzed in this work are expected to have low concentration of Cs, 1 mg/mL AMP and the syringe filter were selected as the most optimal methods to use in further optimization and soil sample analysis.

3.1.3 Digestion optimization

As previous experiments tested the radiochemical separation with different separation methods using a simulated solution, the next step was to test the method for a more environmentally relevant matrix by using ^{137}Cs contaminated Fukushima soil samples. The radiochemical separation method described above requires the sample to be in liquid phase to

go through the different steps, thus the Fukushima soil samples must be digested.

Consequently, it was necessary to test the digestion method for soil samples by evaluating the recovery of ^{137}Cs after the full radiochemical separation. In this case, two different acid mixtures were tested and, based on the best recovery of ^{137}Cs and which one was the easiest to work with, an acid mixture was chosen to be used for the rest of the Fukushima samples.

The first acid mix to be tested consisted of only 5 mL ultrapure, concentrated HNO_3 . This acid was chosen for its high ability to digest, broad laboratory accessibility and relatively easiness to use (i.e., under common safety laboratory practice). The second acid mix consisted of 2.5 mL HNO_3 , 5 mL H_3PO_4 and 2.5 mL HBF_4 , all concentrated. In theory, this acid mix provided a better digestion efficiency of soil samples, but it was relatively harder to work with (due to additional steps as each acid was dispensed individually into the Teflon tubes and extra safety cautions required) and produced more waste compared to acid mix 1.

For the evaluation of digestion recovery, 5 soil samples with different organic content (15-50%) were digested in duplicate, one replicate per acid mix. The ^{137}Cs activity concentration in the soil samples before and after digestion (measured in the NaI-detector) resulted in an average ^{137}Cs recovery of $84 \pm 6\%$ and $90 \pm 2\%$ for acid mix 1 and acid mix 2, respectively. The LOD and LOQ of the gamma spectrometry measurements were 0.25 and 0.84 Bq, respectively. Reference materials IAEA-300 and IAEA-373 (Appendix 2) were also measured to verify counting accuracy and were within 5% of the certified value. As predicted, acid mix 2 had a better overall digestion efficiency than acid mix 1. This could also be seen visibly in the digestants; after settling overnight, the bottom of the 15 mL tubes in the acid mix 1 samples contained solid materials (likely to be silicate phases) but the solutions were clear in the acid mix 2 samples, indicating full digestion (Figure 3.4). Nevertheless, acid mix 1 had an acceptable level of recovery, with the upper range overlapping with the acid mix 2 recovery. Moreover, concentrate HNO_3 was much easier to work with than a mixture of nitric-, phosphoric- and fluoroboric acids. Therefore, acid mix 1 was chosen to be used in further experiments.

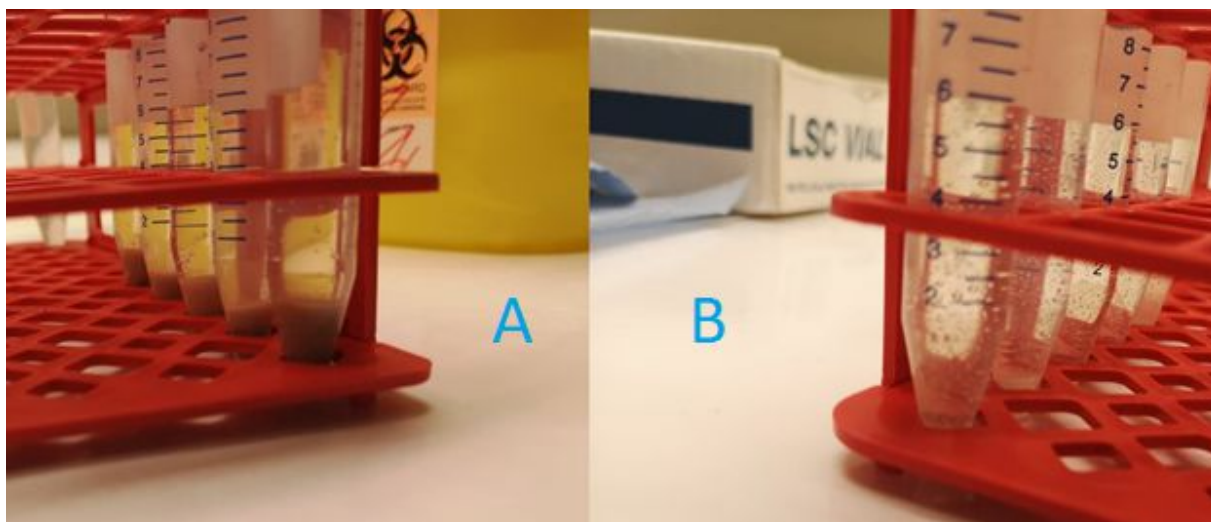


Figure 3. 4: Photo of soil samples after acid microwave digestion: (A) with acid mix 1 (only HNO_3) and (B) with acid mix 2 (HNO_3 , H_3PO_4 and HBF_4). The dark solids in the bottom of tubes in (A) are undigested sample materials.

3.1.4 Digestion and radiochemical separation optimization

Once the extraction of ^{137}Cs from soils by acid digestion had been checked, it was important to evaluate the steps of the radiochemical separation when using digested soil samples. Previous results showed data from step 1+2 and step 1+2+3 but did not determine whether step 2, the anion resin, was a determining factor of the radiochemical separation (in Table 3.1 only the “syringe 1-10 AMP” samples were obtained using step 1 and 3). Therefore, step 2 was tested for the soils samples to know if it is necessary for the radiochemical separation or if it could be skipped to reduce the experimental time but without affecting the ICP-MS measurement. Step 2 would be necessary if using only steps 1 and 3 result in high concentrations of elements that could interfere with the measurement of radiocesium and/or contaminate the instrument compromising later use. An example of contamination is Mo, which can prove hard to remove from the instrument if injected in high concentrations. Since 61% of the AMP consists of Mo, it is important to keep the concentration of this ion in the matrix as low as possible. It is also important to remove Ba due to the isobaric interferences with both ^{135}Cs and ^{137}Cs .

The necessity of step 2 was tested by using 6 replicates of the same soil sample divided into two groups, where one group of 3 replicates underwent the full radiochemical separation, whilst the other group of 3 replicates skipped step 2, meaning only steps 1 and 3 of the radiochemical

separation were applied. The final samples were measured for Mo, Ba, Na, Mg, Al, P, Fe, and Rb. Table 3.2 shows the concentrations (in $\mu\text{g/L}$) for various elements of interest. The concentration of Mo was 8.6 ± 5.8 and 121 ± 17 $\mu\text{g/L}$ for step 1+2+3 and for no step 2, respectively, i.e., 10-15 times higher without step 2. For Ba, the measured concentrations were similar, with ~ 1.9 and 1.7 $\mu\text{g/L}$ for step 1+2+3 and no step 2, respectively. The concentration of Na was about two times higher for step 1+2+3 than for no step 2 (ca. 198 and 102 $\mu\text{g/L}$, respectively); whereas for Mg, no step 2 resulted in twice the concentration than step 1+2+3 (ca. 122 and 67 $\mu\text{g/L}$, respectively). Aluminum was at a very similar concentration in samples from both step 1+2+3 and no step 2, with concentrations at ca. 70 $\mu\text{g/L}$, and the same applied to the measured concentrations of P (22-23 $\mu\text{g/L}$), Fe (12-13 $\mu\text{g/L}$), and Rb (684-698 $\mu\text{g/L}$).

Table 3. 2: Concentrations (and 1 standard deviation) of elements of interest to evaluate step 2 when using soil samples. Three replicates of a soil sample underwent the full radiochemical separation (Step 1+2+3) and 3 replicates underwent the radiochemical separation without step 2 (No step 2).

Concentration, $\mu\text{g/L}$								
Samples	Mo	Ba	Na	Mg	Al	P	Fe	Rb
Step 1+2+3	8.6 ± 5.8	1.9 ± 0.2	198 ± 13	67.5 ± 7.2	70.5 ± 8.3	22.9 ± 7.9	13.7 ± 0.2	684 ± 34
No step 2 (step 1+3)	121 ± 17	1.66 ± 0.03	102 ± 23	122 ± 44	70.7 ± 11.9	22.0 ± 7.5	12.1 ± 2.6	698 ± 81

Barium, Al, P, Fe and Rb were in very similar concentrations for both step 1+2+3 and no step 2, whereas Mo was the element with the biggest difference between procedures, as skipping step 2 resulted in 10 to 15 times increase in concentration. Skipping step 2 also had an impact on Mg, as the concentration was doubled than after the full separation. Contrastingly, the opposite happened for Na, where the concentration was twice as much after all 3 steps of the radiochemical separation. The concentration of these elements (Na, Mg, Al and P), however, was low enough to not interfere with the ICP-MS measurements of digested soil samples. Rubidium was initially measured for consideration as an internal standard for the ICP-MS measurements. Unfortunately, the concentrations in the final samples were high and it could not be used.

Even though skipping step 2 had a major impact on the concentration of Mo, the concentration was low enough for it not to contaminate the instrument. On the other hand, the Ba concentrations were very low but very similar for step 1+2+3 and no step 2 samples, meaning that the step 2 of the radiochemical separation (i.e., the anion exchange resin) had a minor effect on the removal of Ba from solution, which happened mainly in step 3 (i.e., the cation exchange resin).

These tests applying the radiochemical separation with step 1+2+3 and no step 2 also allowed to check the effect of the matrix on the recovery of ^{137}Cs . The recovery of ^{137}Cs from the soil sample after digestion was $80 \pm 1.6\%$ for the 6 replicates (measured in the NaI-detector). This recovery was used to calculate the initial ^{137}Cs concentration present in the digested sample undergoing the radiochemical separation. After the radiochemical separation the recovery was $99 \pm 1\%$ and $105 \pm 2\%$ for step 1+2+3 and no step 2, respectively, with 3 replicates each (measured by ICP-MS). This means that the recovery for both methods was satisfactory; yet, skipping step 2 provided a slightly better recovery. This could be because adding an extra step (i.e., step 2) could cause loss of the analyte due to transferring of sample from one column to another. Furthermore, higher concentrations of anions in the matrix due to skipping step 2 seemed to not interfere with the Cs measurement, and the method's LOD for ^{137}Cs was 3.46 pg/L (11 Bq/L), giving a LOQ of 11.5 pg/L (37 Bq/L), determined using 6 method blanks. These low concentrations of LOD and LOQ proved satisfactory for further experiments, as some of the contaminated soil samples may have low concentration of ^{137}Cs .

3.1.5 The optimized method

The evaluation of each step of the radiochemical procedure resulted in an optimized method for the preparation of solid environmental samples and direct measurement of ^{135}Cs and ^{137}Cs by ICP-MS (Figure 3.5). Dried soil samples should be checked for ^{137}Cs activity (e.g., in a NaI-detector) before and after microwave acid digestion to determine the recovery of the radiocesium extraction from solid into solution phase. The digested soil sample is then subjected to Cs separation and preconcentration using AMP and a cation exchange resin. The 30 mL eluted sample contains mainly only Cs (i.e., other matrix ions have been removed from

solution) and is ready for determination of radiocesium concentration and isotopic ratio by QQQ-ICP-MS.

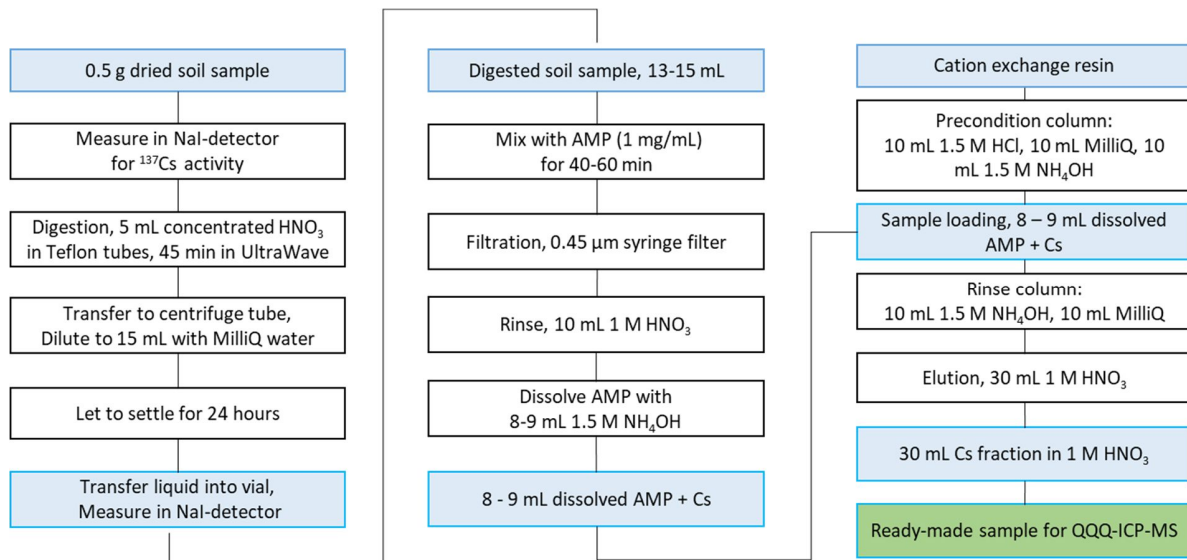


Figure 3. 5: The optimized method for measuring ^{135}Cs in complex soil matrices by QQQ-ICP-MS.

3.2 Isotopic ratio in Fukushima soil samples

3.2.1 Activity concentration of radiocesium

The optimized radiochemical separation and QQQ-ICP-MS analysis (Figure 3.5) was used to obtain the activity concentration and the isotopic ratio of ^{135}Cs and ^{137}Cs (Table 3.3) in Fukushima soil samples (Table 2.3). The digestion of the 13 different soil samples (3 replicates each) resulted in an average recovery of $75 \pm 4\%$ for ^{137}Cs ($n = 39$). This average recovery is in accordance with the recovery obtained during the method optimization ($84 \pm 6\%$) but slightly lower. During the method optimization only 5 different soil samples were tested, whilst this average recovery was obtained from 13 different soil samples with a wider range in organic matter content, type of soil, and location of sampling sites. Moreover, the reason for not a full recovery could be because not everything in the sample was fully digested using the acid mix 1. As shown in Figure 3.4, clearly some soil material remained at the bottom of the tubes, meaning that some of the Cs could be trapped within less insoluble, inert particles such as silicates and/or Cs-containing particles (Reinoso-Maset et al., 2020; Tetteh, 2018). Nevertheless, a 75% average recovery is satisfactory as there is enough recovered Cs, even for samples at low concentrations, to get through the radiochemical separation and ICP-MS

measurement. After the radiochemical separation (step 1+3), the recovery of ^{133}Cs and ^{137}Cs were in average $100 \pm 3.5\%$ and $97 \pm 2.9\%$, respectively ($n = 60$ replicates). Out of these replicates, 39 derived from the digested bulk soils (13 samples x 3 replicates), whereas the other 21 were sequential extraction leachates (7 samples x 3 replicates). In both cases the matrix of the samples had low pH-levels, meaning that the sorption of Cs on the AMP was favorable with only 1 mg/mL AMP. The average recovery for both isotopes in the soil samples are within the same range obtained during the method optimization and during the evaluation of step 2 in section 3.1.4.

The soil samples (Table 3.3) were collected within 4 general sampling sites located at different distances in different directions from the FDNNP reactors (Figure 3.10), thus the measured activity concentrations of ^{137}Cs varied as expected (all above the method's LOD and LOQ of 2.9 and 9.5 pg/L, respectively (9.3 and 30.5 Bq/L)). The soil corresponding to the sampling site closest to the reactor at 1291 m away from the reactor (sample 14) presented the greatest ^{137}Cs activity concentration of all bulk soil samples, with an average of ~ 3800 Bq/g (Figure 3.6). Moving further away from the reactors, sampling sites within 1375 m and 2371 m (ordered by increasing distance: 3, 1b, 8, 16b, 16c, 16n, 7a, 6a) showed lower activity levels between 60 and 570 Bq/g of bulk soil samples. Contrastingly, samples 17-3 and 17-v collected at the furthest away point from the reactor, at 10561 m, presented significantly higher activity concentrations (1650-1750 Bq/g) than samples collected at closer locations (with exception of sample 14; Figure 3.6). Interestingly, samples 9b and 10c collected at ~ 7800 m from the reactor showed the lowest activity concentration of all the bulk samples (10 -30 Bq/g). These activity concentrations were within values previously reported for the same soil samples used in this study (Reinoso-Maset et al., 2020). Moreover, UNSCEAR and Tsuruta et al. reports show ^{137}Cs deposition maps (Tsuruta et al., 2014; UNSCEAR, 2014), where the highest density of ^{137}Cs was in the close proximity of the FDNPP and branched out northwest-ward, corresponding with the findings in this study, i.e., the samples with the highest activity were collected from sites near the FDNPP and in a northwest direction. On the other hand, the samples with the lowest activity were taken ~ 7800 m in a south-western direction, corresponding well with the reported deposition density maps (Saito et al., 2015)

The difference between activity levels can be explained by the weather conditions at the time of the accident. Days after the accident, the wind blew eastward, making most of the radioactive fallout go into the Pacific Ocean. However, over the course of several days, the weather and terrain conditions and winds affected the atmospheric air polluted masses, giving the northern, north-western, and southern areas around the FDNPP important deposition plumes of radiocesium (Saito et al., 2015; Tsuruta et al., 2014; UNSCEAR, 2014). This means that the wind direction the days after the accident had a major impact on the deposition of Cs, as showed here by the differences in ^{137}Cs activity for the different soil samples collected in different directions from the reactor (Table 3.3, Figure 3.10). Overall, the activity levels measured in this study are consistent with previous findings and agree with the deposition plumes governed by the changing wind-direction at the time after the accident.

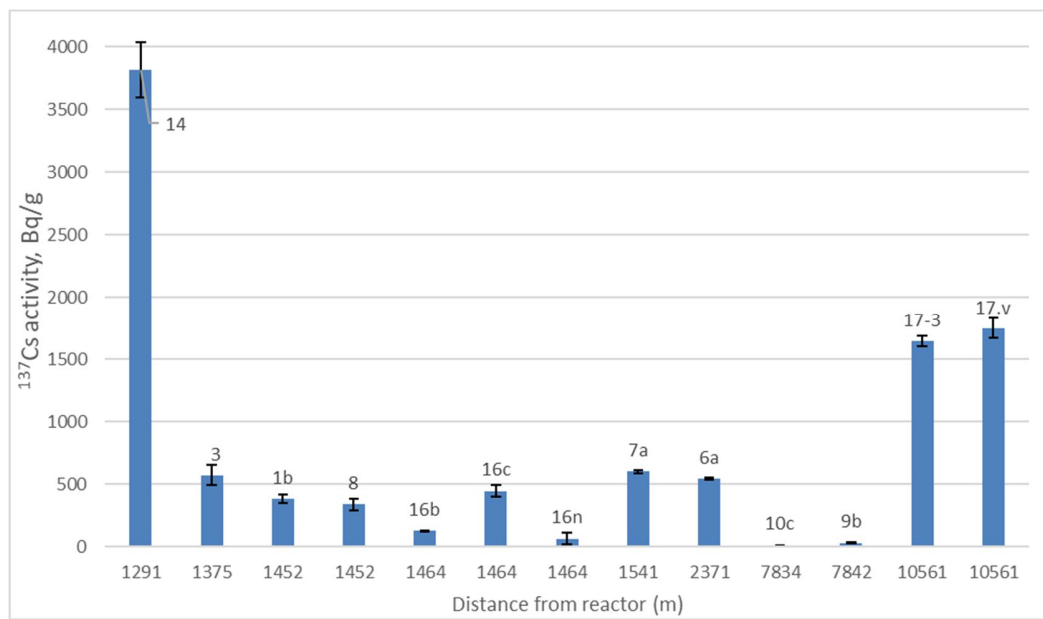


Figure 3. 6: Average activity concentration in Bq/g of ^{137}Cs in digested bulk samples versus the distance from the FDNPP reactors to the sampling sites. Error bars represent 1 standard deviation of triplicate samples. Number on top of bars indicate sampling site. Measured by QQQ-ICP-MS.

Table 3. 3: Results for Fukushima bulk and sequential extraction soil samples. Sampling sites details (distance and wind direction) and average activity concentration of ^{135}Cs and ^{137}Cs as well as the average isotopic ratio of $^{135}\text{Cs}/^{137}\text{Cs}$ with standard deviation and RSD are reported. All data for ^{135}Cs and ^{137}Cs were decay-corrected back to date of accident and corrected for loss in digestion.

Sample details			^{135}Cs , Bq/g			^{137}Cs , Bq/g			$^{135}\text{Cs}/^{137}\text{Cs}$		
Label	Distance, m	Windrose	Average	Stdev	RSD	Average	Stdev	RSD	Average	Stdev	RSD
<i>Bulk soil samples, n = 3</i>											
1b	1452	WNW	0.0018	0.0002	9	383	33	9	0.365	0.003	1
3	1375	WNW	0.0027	0.0004	14	570	79	14	0.354	0.006	2
6a	2371	SSE	0.0025	0.0001	4	542	8	2	0.36	0.01	3
7a	1541	SSE	0.0029	0.0001	2	601	13	2	0.361	0.005	1
8	1452	WNW	0.0016	0.0002	13	338	47	14	0.36	0.01	4
9b	7842	WSW	0.0001	0	14	30	4	13	0.376	0.03	9
10c	7834	WSW	0.0001	0	24	11.2	0.7	7	0.40	0.05	13
14	1291	SSW	0.0179	0.001	5	3816	221	6	0.357	0.002	1
16b	1464	WNW	0.0006	0	0	127	4	3	0.35	0.01	3
16c	1464	WNW	0.0021	0.0002	11	445	47	11	0.36	0.01	3
16n	1464	WNW	0.0003	0	11	63	8	12.3	0.353	0.006	2
17-3	10561	WNW	0.0077	0.0002	3	1645	40	2	0.355	0.002	1
17-v	10561	WNW	0.0082	0.0004	5	1749	79	5	0.356	0.005	1
<i>Sequential extraction samples [step 6, (Fraction 6)], n = 3</i>											
SR1 (7a)	1541	SSE	0.0009	0.0001	8	201	16	8	0.356	0.001	0
HP1 (8)	1452	WNW	0.0006	0.0001	9	135	12	9	0.353	0.001	0
TR1B (10c)	7834	WSW	0	0	1	2.5	0.3	13	0.37	0.06	16
HT2 (13)	1349	SSW	0.0016	0	1	345	7	2	0.357	0.003	1
INP (16b)	1464	WNW	0.0001	0	6	17.2	0.6	3	0.35	0.01	4
INS6 (16n)	1464	WNW	0.0001	0	5	22	1	7	0.35	0.02	5
SUZ (18)	4690	WSW	0.0007	0.0001	13	143	20	14	0.353	0.003	1

Differences in activity concentration in these contaminated soils could also be associated to differences in soil characteristics, e.g., different organic content (Table 2.3). There was a correlation between organic content and activity concentration for most of the samples. A good example is the soil samples collected at site 16, where 16b and 16n contained 127 and 63 Bq/g, respectively, and an organic content of ~8%, while sample 16c with > 30% organic materials showed 3.5-7 times higher ^{137}Cs activity (445 Bq/g; Table 3.3). The correlation between activity concentration and organic content also applied to soils 9b and 10c, which contained low organic content (~3% and 8%, respectively) and low ^{137}Cs activity concentrations (~30 and ~10 Bq/g, respectively), whereas higher organic matter (e.g., ~20% for 1b and ~30% for 3) was associated with higher ^{137}Cs activity concentration in the soils (~380 and 570 Bq/g, respectively). The samples collected at the furthest away site and with high measured ^{137}Cs activity levels > 1600 Bq/g (i.e., 17-3 and 17-v) were also characterized by high organic content of $\geq 50\%$ (Table 2.3; Reinoso-Maset et al. (2020)). Nevertheless, there was also a sample containing low organic content (5%) but still presented relatively high activity concentration (~600 Bq/g, sample 7a, Table 3.3). This contradicting result might be explained by the characteristics of the sample, which was composed of soil, gravel, clay, and sand and presented the highest clay fraction of all samples used in this study, i.e., 10% vs. the 0.04 - 4.1% measured for the other samples (Reinoso-Maset et al., 2020). Several studies using electron microscopy suggested that radioactive cesium was fixed to clay minerals rather than organic matter due to the strong binding affinity of these mineral phases and Cs atoms will thus not desorb easily, e.g., more than 70% of the total Cs in the soil profile was absorbed by mica, chlorite and smectite (Kaneko et al., 2015; Mukai et al., 2014). Our results thus confirm that clay and organic materials in the soil might significantly control the retention of Cs, while also preventing downward migration into the soil profile (Kaneko et al., 2015). Studies also found that 80%-90% of the ^{137}Cs activity was retained in the top 2 -4 cm layer of soil profiles in the FDNPP area, with a substantial decrease in activity levels within deeper layers on the soil (Kaneko et al., 2015; Kato et al., 2012; Matsuda et al., 2015), which agrees with the relatively high ^{137}Cs concentration measured in the top-layer soils used in this study (<6 cm, Table 2.3). Overall, considering the soil characterization, wind direction, and distance from reactor combined with

published ^{137}Cs deposition maps, the ^{137}Cs activity of the bulk samples in this study are in good agreement with earlier reports.

The ^{137}Cs activity concentration was also measured in the sequential extraction samples (Table 3.3; Figure 3.7A) and, in general, was significantly lower than the activity concentrations of the bulk samples. Sequential extraction samples with a corresponding bulk sample also measured within this study (i.e., 7a, 8, 10c, 16n and 16b) presented between ~15 and 35% of the ^{137}Cs activity in the counterpart bulk samples. The other sequential extraction samples, i.e., Tetteh (2018) reported the total ^{137}Cs activity concentration to be 390 ± 21 , 186 ± 8 , 5 ± 1 , 139 ± 50 , 680 ± 2 and 232 ± 45 Bq/g for sequential extraction samples from site 7a, 8, 10c, 13, 16b and 18 respectively. Comparing these results with the sequential extraction samples in table 3.3, the ^{137}Cs activity reported in Tetteh (2018) are 40 to 50% higher activity than the sequential extraction samples measured in this study. The sequential extraction samples measured in this study are the fractions resulting from step 6 of sequential extraction carried out by Tetteh (2018), which involved reacting the soils with 7 M HNO_3 at 80 °C for 6 hours. Tetteh's study showed that up to 55% of the ^{137}Cs remained in the residue after the 6-step leaching procedure, i.e., sequential extraction steps 1 to 5 extracted < 20% of the total ^{137}Cs (reversibly bound Cs), step 6 extracted 43-87% (irreversibly bound Cs) and the rest was found in an inert form. The measured sequential extraction samples in this study were therefore expected to have a lower ^{137}Cs activity than the total ^{137}Cs activity concentration in Tetteh (2018) because of the ^{137}Cs activity concentration being extracted in earlier steps (F1 to F5) and also irreversibly bound in the residue following step 6 (F6) sequential extraction.

Although the optimized method in this study (concentrated HNO_3 in an UltraWave microwave system) generally digests mineral phases to a better extent than leaching with 7 M HNO_3 on a sand bath at 80°C, it resulted in an incomplete digestion (Figure 3.4) and extraction of Cs from the Fukushima bulk soils (75 ± 4 % recovery), which can be explained by the reported association of Cs with an inert fraction in the soils, such as Cs-containing particles (Reinoso-Maset et al., 2020).

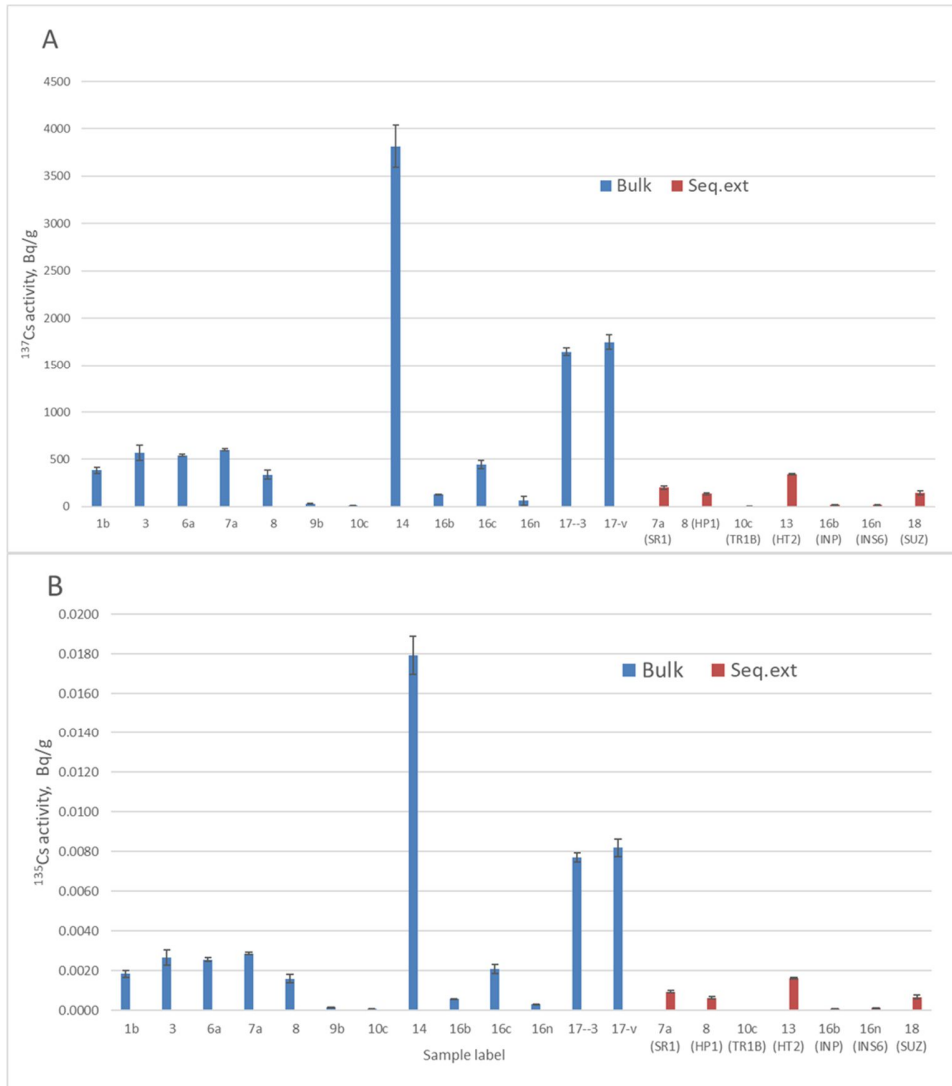


Figure 3. 7: Average ¹³⁷Cs (A) and ¹³⁵Cs (B) activity concentration (in Bq/g) for Fukushima bulk and sequential extraction triplicate soil samples after radiochemical separation without step 2, measured by ICP-MS. Sample labels indicate sampling location within the Fukushima exclusion zone (Table 2.3). Error bars represent 1 standard deviation of triplicate samples.

The activity concentration of ¹³⁵Cs was low for all bulk soil and sequential extraction samples, yet detectable and above the method's LOD and LOQ for ¹³⁵Cs at 2.1 and 7.1 pg/L, respectively ($8.9 \cdot 10^{-5}$ and $3.0 \cdot 10^{-4}$ Bq/L). Although the activity concentrations were low, the same general trend as the ¹³⁷Cs activity concentration was observed (Figure 7A and 7B). For example, samples 14 and 17-v presented the highest activity of ¹³⁷Cs thus, as expected, they presented the highest measured ¹³⁵Cs activity concentrations at 0.002 and 0.0082 Bq/g, respectively. Similar values have been reported in other studies, with ¹³⁵Cs activity concentrations between 0.00025

and 0.0005 Bq/g from soil samples in the FDNPP area (Yang et al., 2016). These low values in activity were expected, as ^{135}Cs has a half-life of 2.3×10^6 years and is a low energy beta-emitter (Zheng et al., 2014a). Nevertheless, the radiochemical separation after digestion and measurement by QQQ-ICP-MS was a suitable method to determine ^{135}Cs in contaminated environmental samples.

3.2.2 $^{135}\text{Cs}/^{137}\text{Cs}$ isotopic ratio in contaminated soils from Fukushima exclusion zone

The isotopic ratio of $^{135}\text{Cs}/^{137}\text{Cs}$ was in the range of 0.35 to 0.40 for both bulk soil and sequential extraction samples (Table 3.3). The uncertainty of the measurements varied among samples, being most RSD values acceptable, i.e., < 5% for 5-7 replicate measurements for each triplicate sample. Samples 9b and 10c (bulk and sequential extraction samples) were the only samples with RSD values over 5%, but these samples also had the lowest ^{135}Cs and ^{137}Cs activity concentrations, explaining the less satisfactory reproducibility. Contrastingly, higher activity concentration (> 30 Bq/g for ^{137}Cs) resulted in substantially less uncertainty in the isotopic ratio of replicate samples. Yet, an increase in activity concentration did not necessarily lower the uncertainty between measurements. Several samples with low RSD (1-2%) had lower activity concentrations than samples with higher RSD (3-5%) (Table 3.3), meaning that activity concentration was not directly linked to the uncertainty of the isotopic ratio measurement. This could indicate that the soil samples were heterogeneous due to the presence of radioactive particles, as reported by Reinoso-Maset et al. (2020) studying the same Fukushima soil samples. Here, although the bulk soils were homogenized by thoroughly mixing before subsampling, differences in particle size and amount of litter were visible in the materials and could have resulted in small differences between the 3 replicates, with a potential associated differences in radioactive particle content. This heterogenous distribution between replicates might hence affected the reproducibility of the activity concentration measurements. However, when comparing the isotopic ratio between replicates, no significant differences were observed, and values were within the range of measurements (see box plot in Appendix 3). In general, low activity concentration (i.e., < 30 Bq/g for bulk and < 25 Bq/g for sequential extraction samples) led to higher RSD values, implying that activity concentrations higher than those are required for this optimized QQQ-ICP-MS method to provide acceptable statistical data.

The $^{135}\text{Cs}/^{137}\text{Cs}$ isotopic ratio could be used to identify the source of Cs that caused the radioactive contamination after the Fukushima accident. Figure 3.8 shows the isotopic ratios measured in the soil samples versus distance and direction of the sampling site from FDNPP and Figure 3.9 shows the location of these sampling sites on a Fukushima exclusion zone map overview. No significant differences in isotopic ratio were observed based solely on distance from the reactors, except for samples collected at ~ 7800 m (i.e., samples 9b and 10c), which presented average isotopic ratios > 0.37 but were also the samples with the highest measurement uncertainty between replicates and lowest activity concentration. Based on direction, samples collected in the WNW and SSE/SSW directions and in proximity of the FDNPP showed similar average isotopic ratios ranging from ~ 0.345 to 0.365 , with the SSE/SSW samples having less variation in isotopic ratio than the WNW samples. The samples collected at ~ 10 km from the reactor (i.e., samples 17-3 and 17-v) showed an average isotopic ratio of ~ 0.355 with very low uncertainty between replicates ($< 1\%$ RSD, Table 3.3). Since the results could not clearly indicate differences in the measured isotopic ratio based on direction, the fallout in each area might have derived from different reactor cores. According to published data, the $^{135}\text{Cs}/^{137}\text{Cs}$ isotopic ratio in the core of reactor units 1, 2 and 3 at the time of the accident were estimated to be ~ 0.39 , ~ 0.35 and ~ 0.34 respectively (Kurihara et al., 2020; Snow et al., 2016). These are very distinctive and specific isotope ratios as, for example, that originated from Chernobyl accident (decay-corrected to 11th of March 2021) was determined to be ~ 0.5 $^{135}\text{Cs}/^{137}\text{Cs}$ (Zok et al., 2021). The $^{135}\text{Cs}/^{137}\text{Cs}$ isotopic ratios measured by QQQ-ICP-MS have been reported to be between 0.34 to 0.35 in soil samples about 20 to 60 km north-west of FDNPP (Yang et al., 2016), 0.375 and 0.355 (Zheng et al., 2014a) in soils collected 20 km south and 230 km south-west of FDNPP, and 0.378 ± 0.0023 in a reference material composed of soil from the FDNPP area (Zheng et al., 2016). In these studies, the $^{135}\text{Cs}/^{137}\text{Cs}$ was preferred over the $^{134}\text{Cs}/^{137}\text{Cs}$ isotopic ratio since ^{134}Cs has a relatively low half-life compared to ^{135}Cs and consequently identification of the source might be inconclusive long time after the accident, as shown for the same soil samples used in this study (Reinoso-Maset et al., 2020). In that work, the isotopic ratio showed a great associated uncertainty due to very low ^{134}Cs activity concentrations in the soils and sediments. Here, the measurement of $^{135}\text{Cs}/^{137}\text{Cs}$ might provide

further information on where the contamination derived from in the Fukushima accident fallout. Yet, there was not a clear trend connecting isotopic ratio and direction (Figure 3.8 and 3.9). Snow et al. (2016) suggested that deposition in the SW direction from FDNPP was a mixture of radiocesium from all 3 cores, reporting $^{135}\text{Cs}/^{137}\text{Cs}$ isotopic ratios between ~ 0.35 and ~ 0.40 , as well as in areas in a NW direction, where measured $^{135}\text{Cs}/^{137}\text{Cs}$ isotopic ratios ranged between ~ 0.34 and ~ 0.36 . Therefore, the isotopic ratios of Fukushima soils measured here are generally in good agreement with reported values and indicate that the radiocesium deposition occurred due to the different release plumes during the accident.

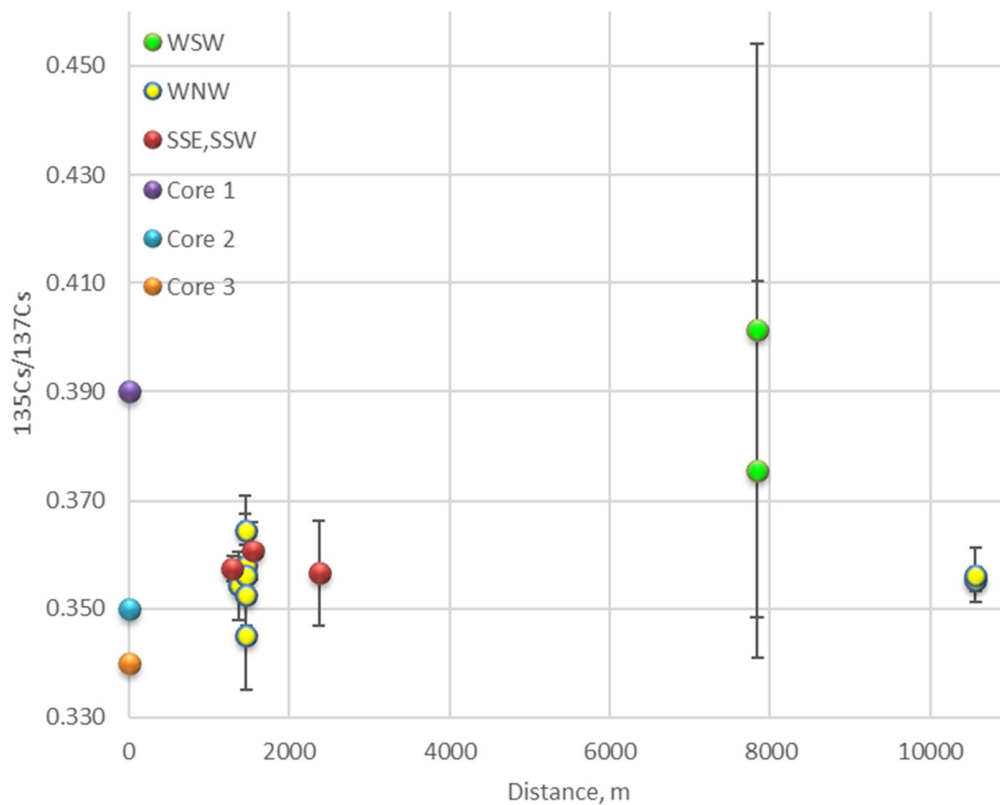


Figure 3. 8: Average isotopic ratio of $^{135}\text{Cs}/^{137}\text{Cs}$ measured in bulk soil samples as a function of distance of the sampling site from the reactor. Color code indicates the direction of the sampling site respect to the reactor (i.e., WSW = west-south-west, WNW = west-northwest, SSE = south-south-east and SSW = south-south-west). Error bars represent 1 standard deviation of 5-7 replicate measurements on 3 replicate samples. The $^{135}\text{Cs}/^{137}\text{Cs}$ isotopic ratio of reactor cores 1, 2 and 3 at the time of the accident are also displayed for reference (Kurihara et al., 2020; Snow et al., 2016).

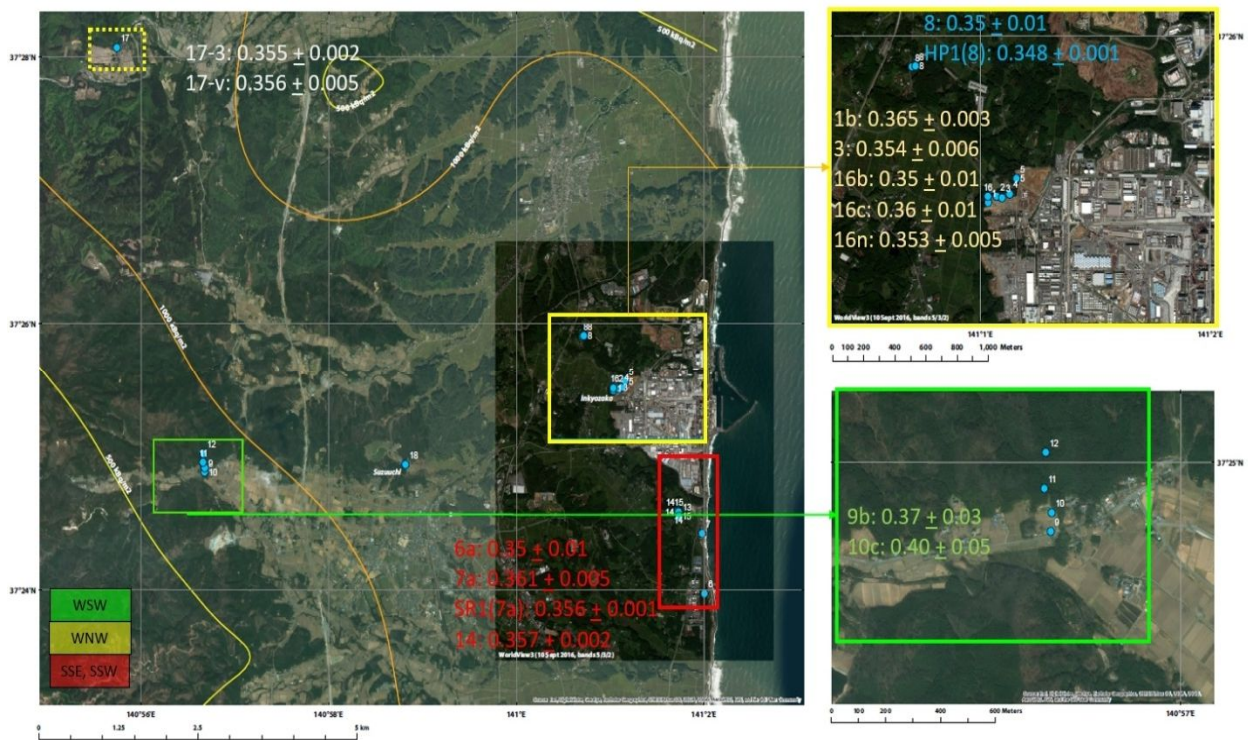


Figure 3. 9: Overview map of the Fukushima landscape including the sampling site locations with the corresponding isotopic ratios of bulk soils (Table 3.3). Color boxes indicate the site direction with respect to the FDNPP reactors. Details of sampling sites and sample characteristics can be found in Table 2.3.

The sequential extraction samples showed $^{135}\text{Cs}/^{137}\text{Cs}$ isotopic ratios of ~ 0.35 (Figure 3.10) and were almost identical to those measured for the bulk samples. For example, identical isotopic ratios were detected for both bulk and sequential extraction samples of soils collected on site 16. Only the 7a and 8 bulk soils had a marginally higher isotopic ratio than the sequential extraction samples, and sample 10c had a higher uncertainty in the isotope ratio (as seen in the bulk) due to the low activity concentrations in this soil. Since these sequential extraction samples derived from chemically leaching the bulk soils without total digestion and there was significant activity left in the residue (Reinoso-Maset et al., 2020; Tetteh, 2018), the comparable isotopic ratios in the bulk soil and sequential extraction samples measured here suggest that the isotopic ratio did not change between the fractions Cs was bound in and that the leached radiocesium potentially has the same origin as the radiocesium remaining in the soil residue.

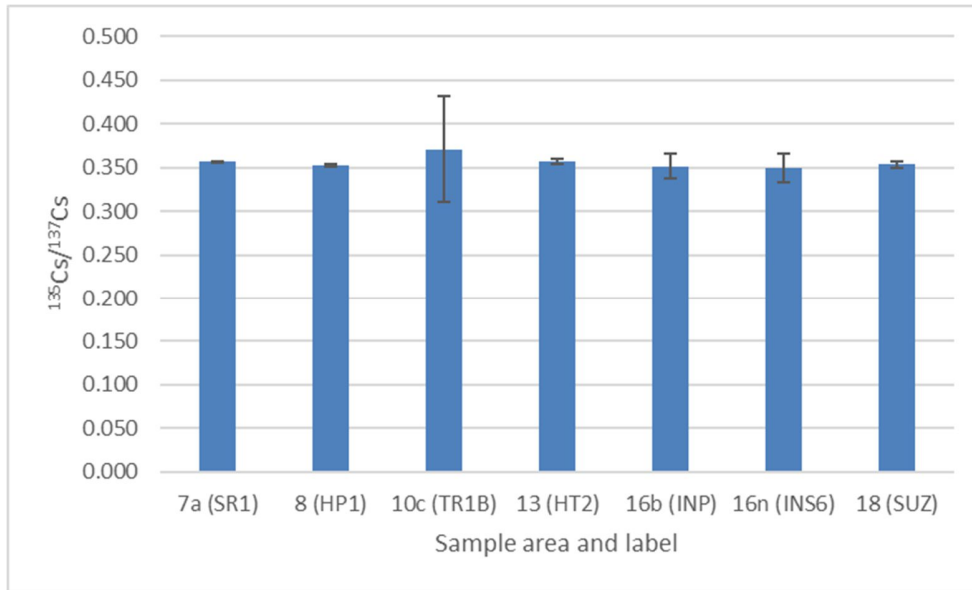


Figure 3. 10: Average isotopic ratio of $^{135}\text{Cs}/^{137}\text{Cs}$ of sequential extraction samples (step 6, F6). Labels indicate from the sampling location within the Fukushima exclusion zone (Table 2.3). Error bars represent 1 standard deviation of 5-7 replicate measurements on 3 replicate samples.

4. Conclusions and further research

The digestion and radiochemical separation method optimized in this study worked well to determine cesium isotopes in contaminated environmental soil samples by ICP-MS. The microwave acid digestion using only HNO₃ resulted in a satisfactory average Cs recovery of 75-85% and thus was selected for further analysis. The radiochemical separation with a first step for Cs extraction using AMP and a syringe filter to separate the AMP-Cs powder from the solution, followed by matrix removal using a cation resin column separated and up-concentrated all the Cs present extracted in the digestion (i.e., ~100% Cs recovery) into a less complex matrix solution (i.e., high DF for all measured elements, with DF of 600-4000 and 1000-5000 for Ba and Mo, respectively). The QQQ-ICP-MS method allowed to detect the extracted radiocesium isotopes ¹³³Cs, ¹³⁵Cs and ¹³⁷Cs, with LOD of 0.9 ng/L, 2.1 pg/L (8.9*10⁻⁵ Bq/L), and 2.9 pg/L (9.3 Bq/L), whereas the corresponding LOQ were 3.1 ng/L, 7.1 pg/L (3.0*10⁻⁴ Bq/L) and 9.5 pg/L (30.5 Bq/L), respectively. These limits were very satisfactory to determine any of the 3 isotopes at low activity concentrations in environmental samples, such as those measured in some of the Fukushima bulk soil and sequential extraction samples. Five bulk samples and 2 of the sequential extraction samples presented relatively low ¹³⁷Cs activity concentrations (< 50 Bq/g) resulting in slightly high uncertainty between replicate samples (i.e., 11-14% RSD); nevertheless, the reproducibility of the whole method was very satisfactory (i.e., activity concentrations were within 2-9% for most samples).

Applying the optimized method allowed to determine the ¹³⁵Cs/¹³⁷Cs isotopic ratio in the Fukushima soils and sequential extraction fractions. This ratio was estimated between ~0.345 to ~0.365 for all samples, with exception to those collected in a WSW direction from the reactor most likely due to low radiocesium activity concentrations measured in soils from this area. The reproducibility of the isotopic ratio measurement was consequently lower in these samples (~15% RSD), but was very good for higher activity concentrations (< 5% RSD). The determined isotopic ratios were in agreement with previously published studies, confirming that the radiocesium contamination derived from radioactive fallout originated during the FDNPP accident. However, the results did not show any clear correlation with distance and direction from the FDNPP that could connect the contamination with the known release plumes and

indicate the source reactor. As seen by other studies, the measured isotope ratios indicate that the radiocesium deposited at these locations is a mixture of radiocesium from the 3 different reactor cores of units 1, 2 and 3. The sequential extraction fractions presented similar $^{135}\text{Cs}/^{137}\text{Cs}$ isotopic ratios to the bulk soil counterpart, suggesting that the irreversibly bound radiocesium in the inert residues had the same origin as the leached radiocesium. Since radioactive particles have been identified as one of the major sources of radiocesium in Fukushima soils and sediments (Reinoso-Maset et al., 2020), further research on source identification using isotopic ratios could include the analysis of single particles (Kurihara et al., 2020).

Overall, this study has shown the importance of $^{135}\text{Cs}/^{137}\text{Cs}$ isotopic ratios as a tool in future research and monitoring of radiocesium contamination in the environment. As ^{134}Cs has a relatively short half-life, using $^{134}\text{Cs}/^{137}\text{Cs}$ isotopic ratio would not be sustainable in the long run due to undetectable ^{134}Cs , whereas the longer half-life of ^{135}Cs allows the determination of $^{135}\text{Cs}/^{137}\text{Cs}$ isotopic ratios by mass spectrometry. Even if this method implies the destruction of the original sample (i.e., digestion and radiochemical separation) and possibly higher costs than radiometric techniques (i.e., gamma vs. mass spectrometry), the sensitivity of the detection was not compromised, it allowed to simultaneously measure cesium isotopes and other stable elements, and the total sample preparation per sample and analysis time was reasonable (i.e., up to ~15 samples digested simultaneously in 1.5 h, 6-12 samples per day for the radiochemical separation, and 100-120 samples per a day run in QQQ-ICP-MS measurements). The optimized method from sample digestion to measurement in the QQQ-ICP-MS provides very low LOD/LOQ as well as good reproducibility for ^{135}Cs and ^{137}Cs activity concentrations and isotopic ratio. Nevertheless, the sensitivity of the detection could be improved by using a more advance introduction system such as the ApexQ-nebulizer, which is more efficient transporting the solution to the plasma and requires small sample volumes (i.e., 0.5 mL vs. 3 mL per sample). Thus, the final fraction in the radiochemical separation could be evaporated and redissolved to a smaller volume, thus increasing the activity concentrations in the samples. Even if this would be at the expense of lengthening the sample preparation time, the chances of detecting low contaminated environmental samples.

References

- The 30-Minute Guide to ICP-MS*. (2004). Perkin Elmer. Available at: https://www.perkinelmer.com/CMSResources/Images/44-74849tch_icpmsthirtyminuteguide.pdf (accessed: 11.29).
- Andersen, O. (2016). Chapter 5 - Decorporation of Radionuclides. In Aaseth, J., Crisponi, G. & Andersen, O. (eds) *Chelation Therapy in the Treatment of Metal Intoxication*, pp. 253-284. Boston: Academic Press.
- Apex Q Desolvating Nebulizer*. (2021). Elemental Scientific. Available at: <https://www.icpms.com/pdfv1/Apex%20Overview%2017162-2.pdf> (accessed: 11.29).
- Aronson, J. K. (2016). Cesium. In Aronson, J. K. (ed.) *Meyler's Side Effects of Drugs (Sixteenth Edition)*, p. 219. Oxford: Elsevier.
- Basuki, T., Miyashita, S., Tsujimoto, M. & Nakashima, S. (2018). Deposition density of ¹³⁴Cs and ¹³⁷Cs and particle size distribution of soil and sediment profile in Hibara Lake area, Fukushima: an investigation of ¹³⁴Cs and ¹³⁷Cs indirect deposition into lake from surrounding area. *Journal of Radioanalytical and Nuclear Chemistry*, 316 (3): 1039-1046. doi: 10.1007/s10967-018-5809-1.
- Chino, M., Terada, H., Nagai, H., Katata, G., Mikami, S., Torii, T., Saito, K. & Nishizawa, Y. (2016). Utilization of ¹³⁴Cs/¹³⁷Cs in the environment to identify the reactor units that caused atmospheric releases during the Fukushima Daiichi accident. *Scientific Reports*, 6 (1): 31376. doi: 10.1038/srep31376.
- Choppin, G., Liljenzin, J.-O., Rydberg, J. & Ekberg, C. (2013). *Radiochemistry and Nuclear Chemistry*. 4 ed.: Elsevier inc.
- Gad, S. C. & Pham, T. (2014). Cesium. In Wexler, P. (ed.) *Encyclopedia of Toxicology (Third Edition)*, pp. 776-778. Oxford: Academic Press.
- IAEA. (2015). *The Fukushima Daiichi Accident*, vol. 4. Vienna: INTERNATIONAL ATOMIC ENERGY AGENCY.
- IAEA. (2021). *Table of Nuclides - Nuclear structure and decay data*: IAEA - Nuclear Data Section. Available at: <https://www-nds.iaea.org/relnsd/vcharthtml/VChartHTML.html> (accessed: 11.29).
- IAEA, D. G. (2015). The Fukushima Daiichi Accident
- Kaneko, M., Iwata, H., Shiotsu, H., Masaki, S., Kawamoto, Y., Yamasaki, S., Nakamatsu, Y., Imoto, J., Furuki, G., Ochiai, A., et al. (2015). Radioactive Cs in the Severely Contaminated Soils Near the Fukushima Daiichi Nuclear Power Plant. *Frontiers in Energy Research*, 3 (37). doi: 10.3389/fenrg.2015.00037.
- Kato, H., Onda, Y. & Teramage, M. (2012). Depth distribution of ¹³⁷Cs, ¹³⁴Cs, and ¹³¹I in soil profile after Fukushima Dai-ichi Nuclear Power Plant Accident. *Journal of Environmental Radioactivity*, 111: 59-64. doi: <https://doi.org/10.1016/j.jenvrad.2011.10.003>.
- Kumar, V., Goel, R., Chawla, R., Silambarasan, M. & Sharma, R. K. (2010). Chemical, biological, radiological, and nuclear decontamination: Recent trends and future perspective. *Journal of pharmacy & bioallied sciences*, 2 (3): 220-238. doi: 10.4103/0975-7406.68505.
- Kurihara, Y., Takahata, N., Yokoyama, T. D., Miura, H., Kon, Y., Takagi, T., Higaki, S., Yamaguchi, N., Sano, Y. & Takahashi, Y. (2020). Isotopic ratios of uranium and caesium in spherical

- radioactive caesium-bearing microparticles derived from the Fukushima Dai-ichi Nuclear Power Plant. *Scientific Reports*, 10 (1): 3281. doi: 10.1038/s41598-020-59933-0.
- Matsuda, N., Mikami, S., Shimoura, S., Takahashi, J., Nakano, M., Shimada, K., Uno, K., Hagiwara, S. & Saito, K. (2015). Depth profiles of radioactive cesium in soil using a scraper plate over a wide area surrounding the Fukushima Dai-ichi Nuclear Power Plant, Japan. *Journal of Environmental Radioactivity*, 139: 427-434. doi: <https://doi.org/10.1016/j.jenvrad.2014.10.001>.
- Miller, C. J. (1995). *Cesium removal from liquid acidic wastes with the primary focus on ammonium molybdophosphate as an ion exchanger: A literature review*. United States.
- Mukai, H., Hatta, T., Kitazawa, H., Yamada, H., Yaita, T. & Kogure, T. (2014). Speciation of Radioactive Soil Particles in the Fukushima Contaminated Area by IP Autoradiography and Microanalyses. *Environmental Science & Technology*, 48 (22): 13053-13059. doi: 10.1021/es502849e.
- NCBI. (2021). *PubChem Compound Summary for CID 5354618, Cesium.*: National Center for Biotechnology Information. Available at: <https://pubchem.ncbi.nlm.nih.gov/compound/Cesium> (accessed: 12.01).
- NRA. (2015). *Radiation Monitoring Information: Monitoring Information of Environmental Radioactivity Level*. Nuclear Regulation Authority. Available at: <https://radioactivity.nsr.go.jp/ja/list/191/list-1.html> (accessed: 11.29).
- Radaram, B., Mako, T. & Levine, M. (2013). Sensitive and selective detection of cesium via fluorescence quenching. *Dalton Transactions*, 42 (46): 16276-16278. doi: 10.1039/C3DT52215F.
- Reinoso-Maset, E. (2020). *KJM350: Radioactivity and radiation protection*. Center for Environmental Radioactivity Department for Environmental Sciences, MINA, NMBU: NMBU.
- Reinoso-Maset, E., Brown, J., Pettersen, M. N., Steenhuisen, F., Tetteh, A., Wada, T., Hinton, T. G., Salbu, B. & Lind, O. C. (2020). Linking heterogeneous distribution of radiocaesium in soils and pond sediments in the Fukushima Daiichi exclusion zone to mobility and potential bioavailability. *Journal of Environmental Radioactivity*, 211: 106080. doi: <https://doi.org/10.1016/j.jenvrad.2019.106080>.
- Russell, B. C., Croudace, I. W., Warwick, P. E. & Milton, J. A. (2014). Determination of Precise ¹³⁵Cs/¹³⁷Cs Ratio in Environmental Samples Using Sector Field Inductively Coupled Plasma Mass Spectrometry. *Analytical Chemistry*, 86 (17): 8719-8726. doi: 10.1021/ac501894a.
- Saito, K., Tanihata, I., Fujiwara, M., Saito, T., Shimoura, S., Otsuka, T., Onda, Y., Hoshi, M., Ikeuchi, Y., Takahashi, F., et al. (2015). Detailed deposition density maps constructed by large-scale soil sampling for gamma-ray emitting radioactive nuclides from the Fukushima Dai-ichi Nuclear Power Plant accident. *Journal of Environmental Radioactivity*, 139: 308-319. doi: <https://doi.org/10.1016/j.jenvrad.2014.02.014>.
- Snow, M. S., Snyder, D. C. & Delmore, J. E. (2016). Fukushima Daiichi reactor source term attribution using cesium isotope ratios from contaminated environmental samples. *Rapid Commun Mass Spectrom*, 30 (4): 523-32. doi: 10.1002/rcm.7468.
- Tetteh, A. (2018). *Speciation and mobility of particle-associated radiocesium in soils and pond sediments from Fukushima, Japan*. Ås, Norway: NMBU.

- Tsuruta, H., Oura, Y., Ebihara, M., Ohara, T. & Nakajima, T. (2014). First retrieval of hourly atmospheric radionuclides just after the Fukushima accident by analyzing filter-tapes of operational air pollution monitoring stations. *Scientific Reports*, 4 (1): 6717. doi: 10.1038/srep06717.
- UNSCEAR. (2014). *UNSCEAR 2013 REPORT VOL. 1*, https://www.unscear.org/docs/publications/2013/UNSCEAR_2013_Report_Vol.I.pdf.
- Yang, G., Tazoe, H. & Yamada, M. (2016). Rapid determination of ¹³⁵Cs and precise ¹³⁵Cs/¹³⁷Cs atomic ratio in environmental samples by single-column chromatography coupled to triple-quadrupole inductively coupled plasma-mass spectrometry. *Analytica Chimica Acta*, 908: 177-184. doi: <https://doi.org/10.1016/j.aca.2015.12.041>.
- Yasunari, T. J., Stohl, A., Hayano, R. S., Burkhardt, J. F., Eckhardt, S. & Yasunari, T. (2011). Cesium-137 deposition and contamination of Japanese soils due to the Fukushima nuclear accident. *Proceedings of the National Academy of Sciences of the United States of America*.
- Zheng, J., Bu, W., Tagami, K., Shikamori, Y., Nakano, K., Uchida, S. & Ishii, N. (2014a). Determination of ¹³⁵Cs and ¹³⁵Cs/¹³⁷Cs Atomic Ratio in Environmental Samples by Combining Ammonium Molybdophosphate (AMP)-Selective Cs Adsorption and Ion-Exchange Chromatographic Separation to Triple-Quadrupole Inductively Coupled Plasma–Mass Spectrometry. *Analytical Chemistry*, 86 (14): 7103-7110. doi: 10.1021/ac501712m.
- Zheng, J., Tagami, K., Bu, W., Uchida, S., Watanabe, Y., Kubota, Y., Fuma, S. & Ihara, S. (2014b). ¹³⁵Cs/¹³⁷Cs Isotopic Ratio as a New Tracer of Radiocesium Released from the Fukushima Nuclear Accident. *Environmental Science & Technology*, 48 (10): 5433-5438. doi: 10.1021/es500403h.
- Zheng, J., Cao, L., Tagami, K. & Uchida, S. (2016). Triple-Quadrupole Inductively Coupled Plasma-Mass Spectrometry with a High-Efficiency Sample Introduction System for Ultratrace Determination of ¹³⁵Cs and ¹³⁷Cs in Environmental Samples at Femtogram Levels. *Analytical Chemistry*, 88 (17): 8772-8779. doi: 10.1021/acs.analchem.6b02150.
- Zok, D., Blenke, T., Reinhard, S., Sprott, S., Kegler, F., Syrbe, L., Querfeld, R., Takagai, Y., Drozdov, V., Chyzhevskiy, I., et al. (2021). Determination of Characteristic vs Anomalous ¹³⁵Cs/¹³⁷Cs Isotopic Ratios in Radioactively Contaminated Environmental Samples. *Environmental Science & Technology*, 55 (8): 4984-4991. doi: 10.1021/acs.est.1c00180.

Appendix

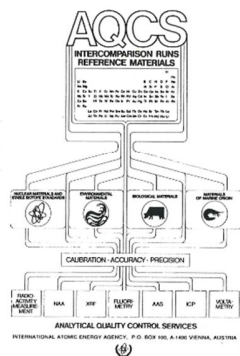
Appendix 1: Element concentration for the simulated solution prepared from the 1643H House standard and different ICP standard solutions.

Simulated Solution	1643H conc	1643H vol	ICP std conc	ICP stand vol	Total vol	Conc in solution
Elements	µg/L	mL	g/L	mL	L	mg/L
Al	141.8	100	10	2	0.2	100.0709
Ba	544.2	100	1	1	0.2	5.2721
Ca	32300	100			0.2	16.15
K	2034	100			0.2	1.017
Mg	8037	100			0.2	4.0185
Mo	121.4	100			0.2	0.0607
Na	20740	100			0.2	10.37
Cs	1	100	0.01	0.2	0.2	0.0105
Sb	58.30	100			0.2	0.02915
As	60.45	100			0.2	0.030225
Be	13.98	100			0.2	6.99*10 ⁻³
B	157.9	100			0.2	0.07895
Cd	6.568	100			0.2	3.284*10 ⁻³
Cr	20.40	100			0.2	0.0102
Co	27.06	100			0.2	0.01353
Cu	22.76	100			0.2	0.01138
Fe	98.1	100			0.2	0.04905
Pb	19.63	100			0.2	9.815*10 ⁻³
Li	17.4	100			0.2	8.7*10 ⁻³
Mn	38.97	100			0.2	0.01949
Ni	62.41	100			0.2	0.031205
Rb	14.14	100			0.2	7.07*10 ⁻³
Se	11.97	100			0.2	5.985*10 ⁻³
Ag	1.062	100			0.2	5.31*10 ⁻⁴
Sr	323.1	100			0.2	0.16155
Te	1.09	100			0.2	5.45*10 ⁻⁴
Tl	7.445	100			0.2	3.7225*10 ⁻³
V	37.86	100			0.2	0.01893
Zn	78.5	100			0.2	0.03925

Appendix 2: Reference materials IAEA-300 and IAEA 373 measuring the efficiency of NaI-detector while doing gamma spectrometry.

REFERENCE SHEET
IAEA-300
 RADIONUCLIDES
 IN
BALTIC SEA SEDIMENT

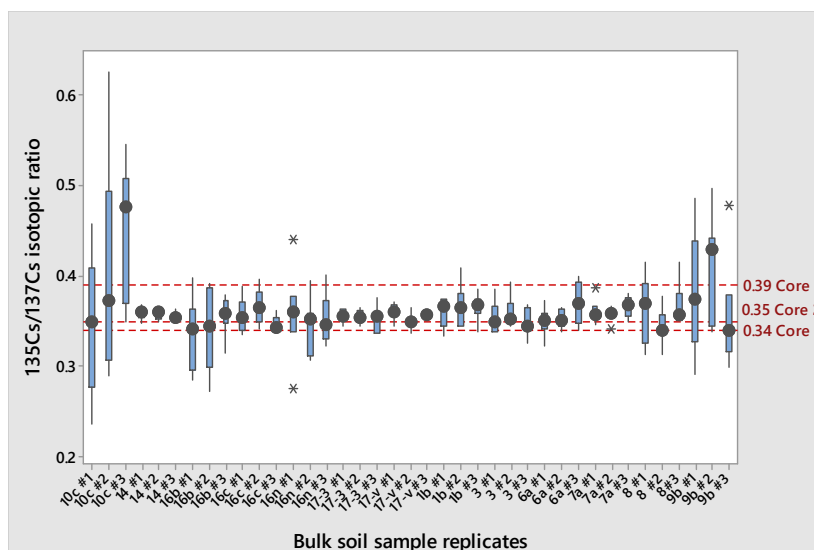
REPORT ON THE
 INTERCOMPARISON RUN IAEA-373: DETERMINATION OF RADIONUCLIDES
 IN GRASS SAMPLE IAEA-373
 V. STRACHNOV, J. LAROSA, R. DEKNER, A. FAJGELI,
 and R. ZEISLER



INTERNATIONAL ATOMIC ENERGY AGENCY
 AGENCY'S LABORATORIES
 ANALYTICAL QUALITY CONTROL SERVICES

Vienna, February 1996

Appendix 3: Box plot of the 7 replicate measurements of $^{135}\text{Cs}/^{137}\text{Cs}$ isotopic ratio for each triplicate sample of the bulk Fukushima soils prepared using the optimized digestion and radiochemical separation followed by QQQ-ICP-MS analysis. Isotopic ratio of the core unit 1, 2 and 3 at the time of the accident are presented by dashed lines.





Norges miljø- og biovitenskapelige universitet
Noregs miljø- og biovitenskapelige universitet
Norwegian University of Life Sciences

Postboks 5003
NO-1432 Ås
Norway